NOAA Technical Memorandum NOS 27

AIRBORNE HYDROGRAPHY SYSTEM LIMITED DESIGN REPORT

Rockville, Md.
January 1978

noaa NATIONAL OCEANIC AND ATMOSPHERIC ADMINISTRATION / National Ocean Survey

NOAA TECHNICAL MEMORANDUMS

National Ocean Survey Series

y (NOS) provides charts and related information for the safe navigation of The survey also furnishes other Earth science data--from geodetic, hydro- eomagnetic, seismologic, gravimetric, and astronomic surveys or observations, rements--to protect life and property and to meet the needs of engineering, dustrial, and defense interests.

NOAA Technical Memorandums NOS series facilitate rapid distribution of material that may be preliminary in nature and which may be published formally elsewhere at a later date. Publications 1 through 8 are in the former series, ESSA Technical Memoranda, Coast and Geodetic Survey Technical Memoranda (C&GSTM). Beginning with 9, publications are now part of the series, NOAA Technical Memorandums NOS.

Publications listed below are available from the National Technical Information Service (NTIS), U.S. Department of Commerce, Sills Bldg., 5285 Port Royal Road, Springfield, VA 22161. Price varies for paper copy; $3.00 microfiche. Order by accession number (in parentheses) when given.

ESSA Technical Memoranda

C&GSTM 1 Preliminary Measurements With a Laser Geodimeter. S. E. Smathers, G. B. Lesley, R. Tomlinson, and H. W. Boyne, November 1966. (PB-174-649)

C&GSTM 2 Table of Meters to Fathoms for Selected Intervals. D. E. Westbrook, November 1966. (PB-174-655)

C&GSTM 3 Electronic Positioning Systems for Surveyors. Angelo A. Ferrara, May 1967. (PB-175-604)

C&GSTM 4 Specifications for Horizontal Control Marks. L. S. Baker, April 1968. (PB-179-343)

C&GSTM 5 Measurement of Ocean Currents by Photogrammetric Methods. Everett H. Ramey, May 1968. (PB-179-083)

C&GSTM 6 Preliminary Results of a Geophysical Study of Portions of the Juan de Fuca Ridge and Blanco Fracture Zone. William G. Melson, December 1969. (PB-189-226)

C&GSTM 7 Error Study for Determination of Center of Mass of the Earth From Pageos Observations. K. R. Koch and H. H. Schmid, January 1970. (PB-190-982)

C&GSTM 8 Performance Tests of Richardson-Type Current Meters: I. Tests 1 Through 7. R. L. Swanson and R. H. Kerley, January 1970. (PB-190-983)

NOAA Technical Memorandums

NOS 9 The Earth's Gravity Field Represented by a Simple Layer Potential From Doppler Tracking of Satellites. Karl-Rudolf Koch and Bertold U. Witte, April 1971. (COM-71-00668)

NOS 10 Evaluation of the Space Optic Monocomparator. Lawrence W. Fritz, June 1971. (COM-71-00768)

NOS 11 Errors of Quadrature Connected With the Simple Layer Model of the Geopotential. Karl-Rudolf Koch, December 1971. (COM-72-10135)

NOS 12 Trends and Variability of Yearly Mean Sea Level 1893-1971. Steacy D. Hicks, March 1973. (COM-73-10670)

NOS 13 Trends and Variability of Yearly Mean Sea Level 1893-1972. Steacy D. Hicks and James E. Crosby, March 1974. (COM-74-11012)

NOS 14 Some Features of the Dynamic Structure of a Deep Estuary. Michael Devine, April 1974. (COM-74-10885)

NOS 15 An Average, Long-Period, Sea-Level Series for the United States. Steacy D. Hicks and James E. Crosby, September 1975. (COM-75-11463)

(Continued on inside back cover)

NOAA Technical Memorandum NOS 27

AIRBORNE HYDROGRAPHY SYSTEM LIMITED DESIGN REPORT

Prepared for
The Engineering Development Laboratory
Office of Marine Technology
National Ocean Survey/NOAA

By
Avco Everett Research Laboratory, Inc.
a subsidiary of Avco Corporation
Everett, Massachusetts

Rockville, Md.
January 1978

UNITED STATES
DEPARTMENT OF COMMERCE
Juanita M. Kreps, Secretary

NATIONAL OCEANIC AND
ATMOSPHERIC ADMINISTRATION
Richard A. Frank, Administrator

National Ocean
Survey
Herbert R. Lippold, Jr., Director

Mention of a commercial company or product does not constitute an endorsement by NOAA National Ocean Survey. Use for publicity or advertising purposes of information from this publication concerning proprietary products or the tests of such products is not authorized.

CONTENTS

List of illustrations v

List of tables vi

Abstract 1

1. Introduction 1

2. Laser hydrography system requirements 2

2.1 Measurement requirements 2

2.2 Performance requirements 2

3. System concept 4

3.1 Optical system concept 4

3.1.1 Concept development 4

3.1.1.1 Scanner concepts 7

3.1.1.2 Laser considerations 10

3.1.1.3 Angular position measurement 12

3.1.2 Description of the optical system concept 13

3.2 Electronics system concept 15

3.2.1 Concept development 15

3.2.2 Description of the electronics system concept 16

4. Performance calculations 16

4.1 Introduction 16

4.2 Radiometric system performance 16

4.2.1 Signal to noise 16

4.3 Eye safety considerations 19

4.4 Horizontal absolute position measurement uncertainty 21

5. Limited system design 22

5.1 Introduction 22

5.2 Optical system. 22
5.2.1 Description of optical system elements 22
5.2.1.1 Optical platform 22
5.2.1.2 Laser. 26
5.2.1.3 Transmitting optics. 26
5.2.1.4 Telescope. 26
5.2.1.5 Field stop and spatial filter. 27
5.2.1.6 Interference filter and collimating optics 27
5.2.1.7 Re-imaging lens and neutral density filter 31
5.2.1.8 Surface return detector. 31
5.2.1.9 Scanner. 32
5.2.1.10 Optical system weight estimates 34
5.2.2 Summary of optical system performance specifications 34
5.3 Electronics system 37
5.3.1 Description of electronics system elements 37
5.3.1.1 Altitude intervalometer. 37
5.3.1.2 Detectors. 39
5.3.1.2.1 Laser output detector. 39
5.3.1.2.2 Surface return detector. 39
5.3.1.2.3 Bottom return detector 39
5.3.1.2.3.1 Photomultiplier gate and gain control. 41
5.3.1.2.4 Detector power supplies. 43
5.3.1.3 Data acquisition system. 43
5.3.1.4 Multiplexer and data buffer. 43
5.3.1.5 Real-time processing 45
5.3.1.5.1 Processor section. 45
5.3.1.5.2 Software development system. 45

5.3.1.6 Recording 46
5.3.1.7 Displays. 46
5.3.1.8 Timing. 46
5.3.1.9 Attitude monitoring unit. 48
5.3.1.10 Aircraft position fixing systems 48
5.3.1.11 Mode status and housekeeping data. 48
5.3.1.12 Laser control. 50
5.3.1.13 Power control and distribution 50
5.3.1.14 Electronics system size, power, and weight estimates 50
5.3.1.15 Preliminary electronics rack layout. 50
5.3.2 Summary of electronics system performance specifications. 50
5.4 Budgetary estimates 54
6. References 54

List of illustrations

Figure

2-1 Spectral diffuse attenuation coefficient. 5
2-2 Signal-to-noise vs. receiver field of view. 5
3-1 Rotating mirror scan pattern produced by AOL system 8
3-2 Single axis oscillating scan pattern. 9
3-3 Two-axis oscillating scan pattern 9
3-4 NOS hydrography system - optical system concept 14
3-5 NOS hydrography system - electronics system concept 14
4-1 Signal-to-noise vs. detection and false alarm probabilities 18
5-1 Optical system layout 24
5-2 Equipment layout in Beechcraft King Air 24
5-3 Cutaway view of Beechcraft King Air 25

5-4 Factors effecting angle of incidence 25
5-5 Wavelength shift due to angle of incidence 29
5-6 Spectral transmission of interference filter 29
5-7 Effect of incident angle on filter transmission. 30
5-8 Scan pattern for conditions shown. 30
5-9 Scan pattern for conditions shown. 33
5-10 Concentrated scan pattern. 33
5-11 Alternate optical system layout. 38
5-12 Electronics system block diagram 38
5-13 Typical grid gating characteristics of ITT F4084 40
5-14 Signal return vs. depth. 40
5-15 Gate and gain control block diagram. 42
5-16 Preliminary electronics rack layout. 52

List of tables

Table

2-1 System measurement requirements. 3
2-2 System performance requirements. 3
2-3 Laser repetition rate vs. altitude and scan angle. 3
3-1 Comparison of candidate lasers 11
4-1 Assumed system, atmospheric and oceanographic parameters 20
5-1 Optical system weight estimates. 35
5-2 Characteristics of FND-100 photodiode. 35
5-3 Characteristics of the RCA 8644 photomultiplier. 35
5-4 Characteristics of the ITT F4084 photomultiplier 35
5-5 Estimated data buffer requirements 44
5-6 Estimated recording requirements 44

5-7 Candidate processing devices 47
5-8 Estimated magnetic tape endurance. 47
5-9 Vertical gyro characteristics. 47
5-10 Directional gyro characteristics 49
5-11 Aircraft position fixing system characteristics. 49
5-12 Electronics system size, power and weight estimates. 49
5-13 Budgetary estimates. 54

AIRBORNE HYDROGRAPHY SYSTEM
LIMITED DESIGN REPORT

Prepared for
The Engineering Development Laboratory
Office of Marine Technology
National Ocean Survey/NOAA

By
Avco Everett Research Laboratory, Inc.
a subsidiary of Avco Corporation
Everett, Massachusetts 02149

ABSTRACT. A limited, hardware design effort has been made for an NOS operational airborne laser hydrographic system. This report describes the resulting system design.

1. INTRODUCTION

This report has been prepared to summarize the efforts of the Avco Everett Research Laboratory, Inc. (AERL), under Contract 7-35373, which had as its purpose the preparation of a limited design of an optimum, prototype, airborne laser hydrography system. This activity was directed toward the technical extrapolation task outlined in the National Ocean Survey (NOS) Laser Hydrography Development Plan. The emphasis in the limited design activity focused on functional system design, sizing, risk assessment, and costing rather than a detailed design from which fabrication could be initiated (ref. 1). In this regard, the technology incorporated in the AERL - developed, NASA Airborne Oceanographic Lidar (AOL) System was assessed for its applicability, as were the results of a joint NOS/Navy - conducted AOL bathymetry flight experiments. Where the technology used in the AOL System was found to meet the requirements of the NOS Laser Hydrography System, it was retained. In those areas where AOL operational performance and field test results indicated that improvements could be made, assessments were conducted to determine optimum, low risk, alternatives, and these were incorporated in the design. Areas in which these improvements have been made are detailed in subsequent sections of this report.

In section 2, the requirements for the NOS Laser Hydrography System are presented and discussed. Section 3 addresses the development of the system concept, design constraints, and the impact of relevant AOL System experience on the design approach chosen. An evaluation of laser candidates is also presented in this section. System performance calculations are discussed in section 4, and the results show that the design parameters chosen will meet the specified system requirements. Finally, the limited design of the NOS Laser Hydrography System is developed in section 5. This section also includes a summary of system performance specifications and budgetary estimates for system implementation. It should be noted here that certain aspects of the signal acquisition scheme incorporated in the design were privately developed

by AERL prior to the initiation of efforts under this Contract and, while included for design enhancement, will not be discussed here. (See section 5.3.1.3.)

In summary, the limited design discussed in this report was developed based on a performance assessment of the AOL System, the most advanced airborne laser bathymetry system in operation. Where improvements were required to enhance performance or meet additional measurement requirements, they were incorporated. The primary objective of the design effort was to optimize the projected performance of the NOS Laser Hydrography System while, at the same time, minimizing development risk, and it is felt that the design presented herein clearly satisfies this goal.

2. LASER HYDROGRAPHY SYSTEM REQUIREMENTS

2.1 Measurement Requirements

At the initiation of the program, the basic measurement requirements for the Laser Hydrography System[1] were reviewed and finalized. They are summarized in table 2-1. The system would be designed for operation with the most commonly encountered coastal water types, including Jerlov Types 1, 3, 5, and 7.[2] As is shown in figure 2-1, the diffuse attenuation coefficient, k, for these waters ranges from ~0.1 m^{-1} to 0.5 m^{-1}. The maximum measurement depth under any given water condition will be dictated by the spectral attenuation coefficient depth product, αD, of 10, where the relationship between k and α is $k=0.2\ \alpha + 0.04\ m^{-1}$. Therefore, under good water conditions, depths in excess of the required 30 m will be easily achievable while under much poorer conditions, say $\alpha = 2\ m^{-1}$, measurements will be limited to ~5 m.

The aircraft identified for use with the system were the Beechcraft King Air 200 T as the primary platform with the DeHaviland Buffalo as a secondary candidate. It is possible that the system might be used in an aircraft which is also configured for photobathymetry; however, such a combination was not to constrain the optimum design of the laser system. The altitude range for laser bathymetry is to be 152 to 914 m with a typical altitude of 304 m (1,000 ft.) specified. The aircraft velocity specified for mapping flights was ~120 nmi/hr., compatible with that necessary for a pilot to maintain a designated flight leg on a mapping pass. The measurement depth range for the system will be 0.3 to 30 m with an $\alpha D=10$. The spatial measurement density required is one data point every 20 m^2, and this is to be achieved at the nominal altitude of 304 m and velocity of 120 nmi/hr. Scanning is required for area coverage, with a scan angle of $\pm 15^{o}$ from nadir desired. The vertical and horizontal accuracies of a measurement are to be $\pm$ 0.3 m and $\pm$ 5 to $\pm$ 7.5 m, respectively, with the latter being chart-scale dependent. The measurement of sea state is also required and the system will be configured to provide aircraft position data. Finally, the system will be designed to operate under both daylight and nighttime background conditions.

2.2 Performance Requirements

Using the measurement requirements discussed in the last section, the performance requirements for the system were developed and are summarized in table 2-2. The laser wavelength required is ~540 nm which, as can be

Table 2-1. System measurement requirements

Laser Wavelength	~540 nm
Laser Bandwidth	~0.1 nm
Laser Pulse Repetition Rate	≥ 500 Hz
Laser Pulse Width	≤ 5 nsec
Probability of Bottom Detection[1]	≥ 99%
Probability of False Alarm[1]	$\leq 10^{-6}$
Amplitude Signal to Noise Ratio[1]	≥ 5.4 at maximum scan angle
Scan Angle	Variable to ~ ± 15° from nadir
Scan Rate	Variable and as required for one data point per 20 m^2
Transmitter Beam Divergence	Variable
Receiver Field-of-View	Variable to 50 mr
Receiver Optical Bandwidth	Minimize consistent with operational and design constraints
Receiver Temporal Resolution	≤ 2.5 nsec
Receiver Dynamic Range	Accept/compensate for signal amplitude variations of ~10^7

1. At an aircraft altitude of 304 m.

Table 2-2. System performance requirements

Application	Bathymetry
Water Types	Jerlov Coastal Types 1, 3, 5 and 7
Aircraft	Fixed wing Beechcraft King Air 200 T - primary DeHaviland Buffalo - secondary
Photobathymetry Combination	Possibly, but not to constrain laser system requirements.
Flight Altitude (photo)	914 to 1, 524 m
Flight Altitude (laser)	152 to 914 m (304 m typical)
Flight Velocity	≥ 120 nmi/hr
Measurement Depth	0.3 to 30 m with an aD = 10
Area Coverage	One data point per 20 m^2 at an aircraft altitude of 304 m and velocity of 120 nmi/hr.
Scan Control	Required; specifics to be driven by platform and design/cost tradeoffs. A scan angle of ± 15° from nadir is desired.
Vertical Measurement Accuracy	± 0.3 m
Horizontal Measurement Accuracy	± 5 to 7.5 m (chart scale dependent)
Sea State	Measurement required
Navigation Data	Range-range
Background Conditions	Day and night operation required

Table 2-3. Laser repetition rate vs. altitude and scan angle

Scan Angle	Altitude				
	152 m	304 m	456 m	609 m	914 m
5°	82	163	244	325	488
10°	164	327	491	655	983
15°	249	497	746	996	1494

seen in figure 2-1, is at the minimum of water attenuation for the coastal types of interest here. A laser bandwidth of $\sim$ 0.1 nm has been specified, primarily to optimally match the peak of the interference filter chosen for use with the system (see section 3). The laser pulse repetition rate required is 500 Hz and was derived from the combination of an aircraft altitude of 304 m, a scan angle of 15^{o}, an aircraft velocity of 120 nmi/hr., and the requirement for one data point every 20 m^2. As can be seen in table 2-3, which was prepared for the aircraft velocity and spatial density parameters specified, the required repetition rate varies with scan angle and aircraft altitude. The laser pulse width required is $\leq$ 5 nsec and is achievable by the lasers under consideration for this application. For good system performance, a false alarm probability of $< 10^{-6}$ and a single pulse detection probability of > 99 percent have been specified. These conditions mandate an amplitude signal-to-noise ratio of at least 5.4 (power signal to noise of $\sim$29). As was mentioned in the last section, a scan angle of $\pm$ 15^{o} from nadir is required for good area coverage and, along with scan rate, is to be variable so as to increase or decrease the mapping density, if desired. The divergence of the laser output beam is to be variable for purposes of optimizing its interaction with the water surface under conditions of varying sea states, as well as to meet eye safety requirements at various aircraft altitudes. With regard to the receiver field of view, the laser beam spreading experiments of Duntley (ref. 3) were assessed, and a simplified model prepared for the water conditions of interest here to relate laser energy received to field of view for an aircraft altitude of 304 m and a water depth of 30 m. The model was then adjusted to present the data in terms of expected signal to noise. The results are shown in figure 2-2. It can be seen from the figure that the signal to noise increases (that is, the effects of increased laser signal outweigh background) as the field of view is increased to 50 mr. For this reason, a maximum receiver field of view of 50 mr has been specified and is required to be variable since, as altitude increases or measurement depth decreases, a smaller setting will be required for purposes of signal-to-noise optimization. The optical bandwidth of the receiver will also have to be minimized for signal-to-noise optimization. A receiver temporal resolution of $\leq$ 2.5 nsec has been specified to be compatible with the $\pm$ 0.3 m vertical measurement accuracy called out in table 2-1, and the receiver must be designed to accept variations in return signal levels of approximately 7 orders of magnitude.

3. SYSTEM CONCEPT

3.1 Optical System Concept

3.1.1 Concept Development

In developing the optical system concept, several important constraints had to be considered. First, it was necessary to provide enough elements in the system to accomplish the depth measuring functions and to identify the parameters which affect the performance and size of the functional units. Important characteristics to be determined here were the necessary collecting aperture and field of view, the required spectral bandpass for good background rejection under daylight conditions, the

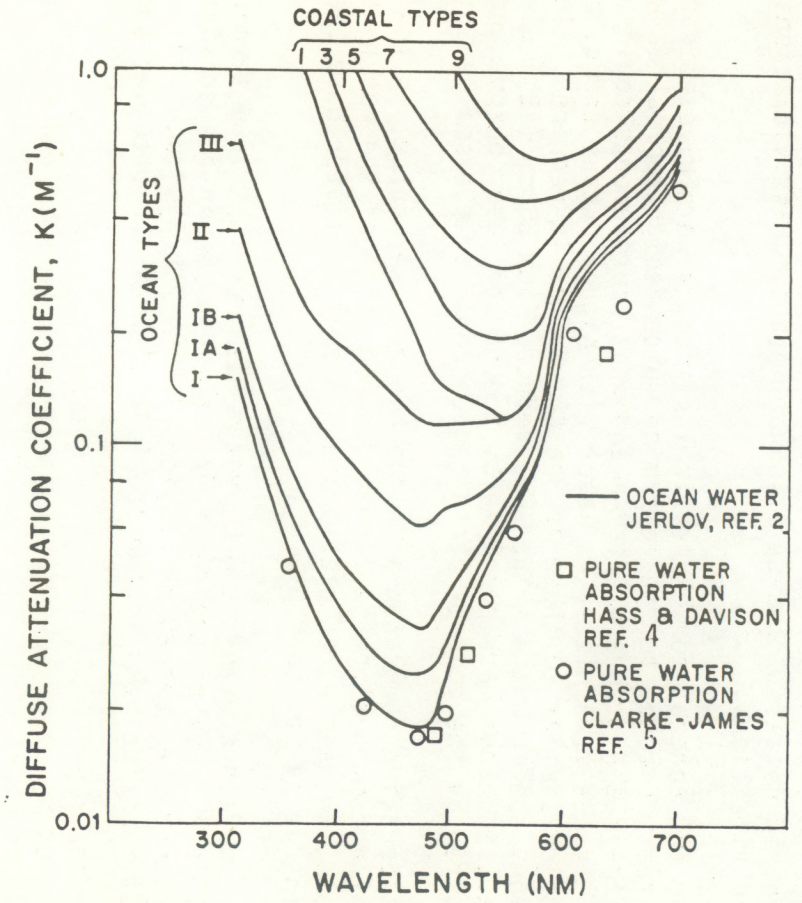

Figure 2-1. Spectral diffuse attenuation coefficient.

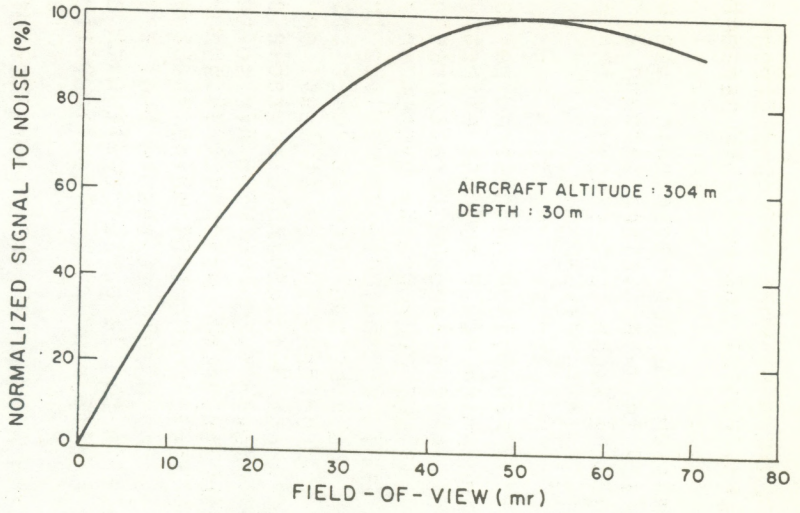

Figure 2-2. Signal-to-noise vs. receiver field of view.

dynamic range required to cover weak bottom returns and strong surface returns, and the necessary adjustments for the variable parameters.

A second major consideration was the method of scanning the output and return beams over the water surface in an efficient pattern with adjustments for varying the rectangularity of the laser spot spacing, the concentration of the scan pattern, and operation with a fixed beam.

A third consideration was that of achieving the desired performance characteristics in a configuration which would be cost effective to construct and operate. The Dehaviland Buffalo is a large aircraft presently operated by NOAA which could accommodate the NOS Hydrography System on a load-sharing basis. The Beechcraft King Air 200T, a candidate to replace the Buffalo, is a much smaller aircraft which could be operated at lower cost but would have to be dedicated to the NOS Hydrography System at least on flights so scheduled. A system concept was adopted involving a portable optical platform which could be readily removed from the King Air so that the aircraft could then be scheduled for photobathymetry missions. This portable approach for the smaller aircraft was the basis for establishing the space constraints for the conceptual design. It is reasonable to assume that a similar configuration would fit equally well in the larger aircraft with appropriate revisions, if necessary, to fit a different window configuration.

The space allocation in the King Air and the configuration of the optical windows in the underside of the aircraft led to the development of a concept that utilizes a single optical platform with all of the optical components rigidly attached to its top surface, including the scanner. The concept, therefore, required detailed consideration of both aircraft vibrations and scanner-induced vibrations.

In developing the concept for the optical system, a careful examination of the AOL System was conducted to determine which design approaches were applicable to the NOS Hydrography System and what improvements could be incorporated. In the transmitter, a laser with higher output energy but with output optics similar to those in the AOL System is required. In the receiver section, the output aperture was reduced from 30 cm (12") dia. to 20 cm (8") dia., a change made possible by the higher laser output and one which was required by the compact packaging concept for the smaller aircraft.

Another consideration connected with the higher laser output is the need for a method of accommodating the larger dynamic range of the return signal. For this purpose, two separate detectors and a spatial filter have been incorporated in the system concept.

Operational experience with the AOL System was important in determining the optimum field of view of the receiver and resulted in a specification of the 50 mr rather than the 20 mr provided in the AOL System. This requirement has ramifications in the specification of the receiver spectral

bandpass because of the dependence of the interference filter transmission on field angle, resulting in a bandpass of over 1.5 nm compared with 0.4 nm in the AOL System. In addition, the AOL System was operated over greater aircraft cabin temperature ranges than originally considered. Since this condition might also be expected with the NOS Hydrography System, a means of controlling interference filter temperature has been incorporated in the concept to minimize the effects of temperature excursions on filter center wavelength and, thus, transmission.

3.1.1.1 Scanner Concepts

The scanner concept was based largely on the satisfactory results achieved with the rotating mirror scanner in the AOL System. Comparisons with other scanners were made, but a strong perference was maintained for the rotating mirror concept because of its dynamic stability, reasonable size, variability, and fairly good spot distribution characteristics. Comparisons were made between oscillating mirror scanners which sweep the beam from side to side and nutating mirror scanners which rotate the beam in an elliptical path around a nadir axis. The latter type is presently being used in the AOL System, and a functional analysis of the design is included in the AOL Final Report.[6] Figure 3-1 depicts the nearly elliptical laser spot pattern produced by a nutating mirror scanner rotating at constant speed.

Oscillating mirror scanners provide a much simpler pattern to analyze but are inherently less stable because of the large acceleration that occurs each time the mirror reverses direction. To minimize the shock at the end of each sweep, a harmonic motion is best employed which causes a bunching of laser spots at the edges of the scan pattern, a characteristic which is present in the elliptical scan pattern as well. If the oscillating concept is used with only one axis of rotation, the scan pattern has the appearance shown in figure 3-2. To make the scan paths more nearly parallel, a second scanning axis is introduced which produces a pattern such as shown in figure 3-3. In this case, both axes of the scanning drive are oscillating in a fixed-phase relationship and both are plotted with harmonic motion to lessen the shock at the points of reversal. The uniformity in spot spacing appears to be satisfactory in the two-axis oscillating scanner and the rotating mirror scanner. An important difference appears when we compare the dynamic characteristics of the oscillating mirror approaches. The various operating conditions of the NOS Hydrography System indicate a need for a variable scan rate between 5-12 Hz with a variable amplitude of $\pm 7.5^{o}$ of mirror motion to scan the optical path $\pm 15^{o}$ from nadir. To oscillate a large mirror at this amplitude and frequency, it is necessary to make the mirror as light as possible to minimize the inertial load. (Lightweight mirrors are available commercially and should be used regardless of the scanner approach chosen.) The oscillatory motion will undoubtedly cause vibrations which can be reduced by means of dynamic balancing provisions in the design. However, these provisions become involved when the design must also include variability in scan angle. It is reasonable to expect that some residual vibration will be inherent in the oscillating drive and that some provisions must be made for isolating the optics from this influence.

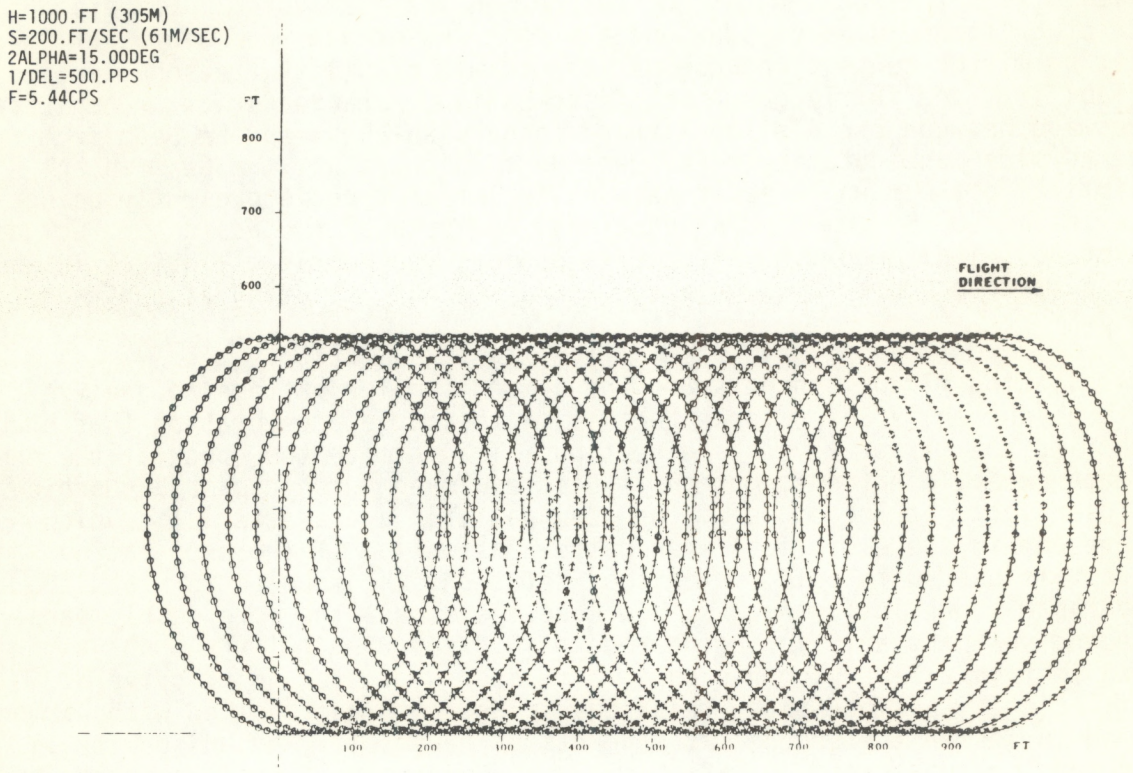

Figure 3-1. Rotating mirror scan pattern produced by AOL system.

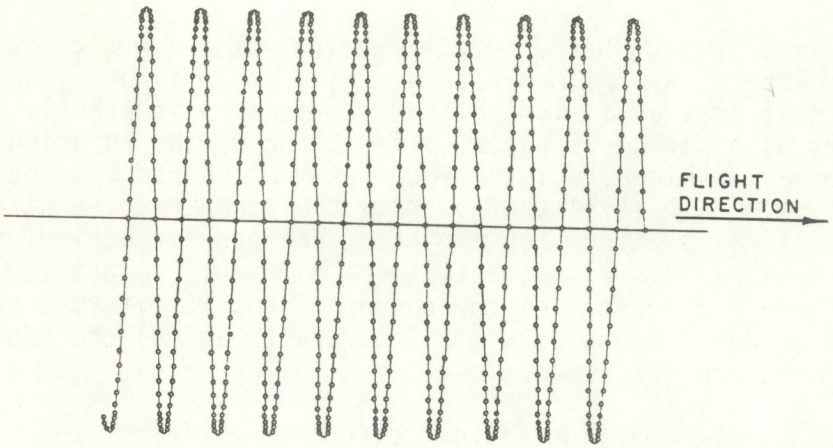

Figure 3-2. Single axis oscillating scan pattern.

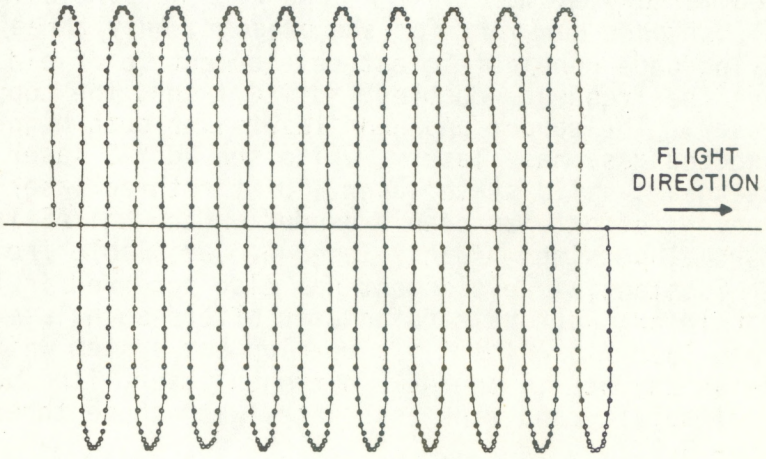

Figure 3-3. Two-axis oscillating scan pattern.

A second concern in an oscillating scanner design is that of measuring the mirror angular motion in a fashion which accurately represents scan angle. The angle measuring device should be rigidly coupled to the mirror assembly, but this is difficult to achieve in an oscillating design.

The rotating mirror design has several practical advantages over the oscillating approaches: a) the moderate weight of the mirror is an advantage because it acts as a flywheel and provides an inherently stable angular velocity; b) a method of dynamically balancing the rotating mirror to a fine degree was developed for the AOL System which reduces the vibrations to a low enough level that permits the scanner to be attached directly to the optical platform, an important feature for achieving metric accuracy and one which will be inherently more difficult to achieve with an oscillating scanner approach; c) the concept lends itself to a reasonable package size and weight for use in a small aircraft; and d) the approach interfaces well with angular readout devices.

For these reasons, the rotating mirror concept is preferred over the oscillating approaches considered. No doubt, an oscillating scanner could be developed with sufficient funding; however, this approach will probably involve a higher risk in achieving the required accuracy because of dynamic instability and also require more space than is available in the King Air Aircraft.

3.1.1.2 Laser Considerations

An important consideration for practical laser hydrography is the choice of lasers. A number of lasers are capable of providing outputs in the green region of the spectrum, that portion which is of interest here. The newly discovered mercury excimer lasers appear to be particularly promising for future applications; however, for the present, only three lasers can be regarded as having undergone sufficient development for field deployment. These lasers are the frequency doubled, Nd:YAG laser, the copper-vapor laser, and the neon laser. The copper and neon lasers are both high gain, electrically excited gas phase lasers, while the Nd:YAG laser is an optically pumped, moderate gain, solid state laser. Of the three lasers, by far the greatest development effort has been expended on the Nd:YAG lasers, and a variety commercial versions of this laser are available from a number of manufacturers. Substantial development has also occurred in the case of the copper-vapor laser, and one manufacturer offers such lasers commercially. The neon laser is primarily a development system which was offered commercially as an adjunct to the AERL nitrogen laser. The performance, size, weight, reliability, and risk associated with these three lasers are compared in table 3-1.

Of the three lasers, the frequency doubled Nd:YAG has achieved by far the greatest output energy per pulse and also the greatest peak power. The copper-vapor laser has demonstrated the highest pulse repetition rate capability but cannot be operated at low repetition rates (< 800 Hz). The 600 Hz capability has not been demonstrated in the neon laser, but based on the nitrogen technology, this laser can presumably also run at 600 Hz.

Table 3-1. Comparison of candidate lasers

	Frequency Doubled Nd:YAG	Copper Vapor	Neon	System Requirement
Pulse Energy[1]	7 mJ	2 mJ	0.7 mJ	1 mJ
Peak Power[1]	390 kW	100 kW	85 kW	200 kW
PRF[1]	400 Hz	4,000 Hz	600 Hz[2]	500 Hz required, > 650 Hz desired
Pulse Duration[1]	18 nsec	20 nsec	8 nsec	≤ 5 nsec
Wavelength	532 nm	510.6 nm	540 nm	~ 540 nm
Beam Quality	5 mr	5 mr	7 mr	≤ 5 mr
Efficiency[3]	0.06%	1.0%	0.012%	Maximize
Volume[4]				
Head	~ 1.3 ft^3	5 ft^3	~ 6.0 ft^3[5]	Small as possible
Power Supply & Control	~ 2.2 ft^3	1.8 ft^3	~ 6.5 ft^3	"
Cooler	~ 2.0 ft^3	5.0 ft^3	~ 12.0 ft^3	"
Total	~ 5.5 ft^3	11.8 ft^3	~ 24.5 ft^3	"
Weight[4]				
Head	~ 55 lb	150 lb	~ 120 lb[5]	Light as possible
Power Supply & Control	~ 80 lb	~ 65 lb	~ 250 lb	"
Cooler	~ 40 lb	~ 50 lb	~ 180 lb.	"
Total	~ 175 lb	~ 265 lb	~ 550 lb.	"
Electrical Power	~ 1,650 W[6]	~ 1,350 W[6]	~ 5,930 W[7]	Minimize
Scalability to Requirements	Pulse shortened by cavity dumping; PRF increase to ~ 600 Hz expected	Pulse shortened by external Pockels cell switching but energy will be less than required (~ 0.5 mJ)	Required pulse energy expected to be difficult to attain	Scalable
Projected Reliability	NADC has achieved good results in an aircraft environment/ Lamp life ~ 10^7 shots	Unknown in aircraft environment/Tube life ~ 10^8 shots	Unknown, must be demonstrated/predecessor has achieved good results in an aircraft environment	Reliable in aircraft environment
Development Risk	Minimal	Minimal for pulse width reduction; unknown for energy increase	Moderate to high for required pulse energy	

Notes:
1. Current state of the art/demonstrated
2. Based on projection, single pulse demonstrated only at 0.7 mJ
3. Laser head only
4. Based on 600 Hz data rate and 1 mJ or state of the art pulse energy whichever is lower except Cu = 2 mJ and 3600 Hz
5. With a 2 meter channel
6. For 600 Hz
7. ~ 8,400 W for 1 mJ pulse energy

In the case of the Nd:YAG laser, most of the commercial units are designed for a higher average power, a higher energy per pulse, and a lower pulse repetition rate than is required here. The performance figures shown in table 3-1 are those pertaining to a frequency doubled Nd:YAG laser developed and flight tested by the Naval Air Development Center (NADC). This laser has a demonstrated capability of 400 Hz but is believed to be easily scalable to the 600 Hz required here. The pulse width, 18 nsec, of the NADC laser is somewhat long for the present purposes, but cavity dumping could be used to shorten the pulse to the requisite 5 nsec with little loss of energy. (The cavity dumping technique has previously been demonstrated on other Nd:YAG lasers.) In the case of the copper-vapor laser, an external Pockels cell shutter must be used to shorten the pulse. Unfortunately, such a technique results in a proportionate decrease in pulse energy. Finally, insofar as laser efficiency is concerned, the copper vapor laser has by far the greatest operating efficiency. However, this advantage is all but lost because of the fact that the laser must be operated at a substantially higher pulse repetition rate than can be used in the present system. As a consequence, the estimated power consumption is little different for the 4000-Hz, copper-vapor laser than for the 600-Hz, Nd:YAG laser. The low-efficiency neon laser would have a significantly greater electrical power consumption than either of the other two.

In terms of configuration, the size and weight of the solid-state Nd:YAG laser is much less than either of the more bulky gaseous systems. In addition, only the Nd:YAG laser has demonstrated reliability in an aircraft environment. The neon laser presently being flown for bathymetry in the AOL System is different in design and much smaller than the neon laser shown in table 3-1. Consequently, the reliability of a scaled up version of the neon laser in an aircraft environment must be regarded as unknown at this time. Finally, the probable success is clearly maximum for the Nd:YAG system. This is a reflection of the greater development effort which has been expended on this laser. On this basis and on the basis of its lighter weight, smaller size and more suitable performance, the frequency doubled Nd:YAG laser is the device of choice for the NOS Hydrography System.

3.1.1.3 Angular Position Measurement

A final major consideration was that of measuring the angular coordinates of the optical path to the spot on the water. This measurement requires provisions for monitoring the motion of the beam directing optics with respect to the local vertical and true north. In the AOL System, an aircraft inertial navigation system (INS) was used as a datum and the accuracy of the measurement was limited by a) the rigidity of the aircraft, b) the flexure in the mounts interfacing the navigator to the aircraft, c) the flexure in the AOL System isolators, and d) the inherent accuracy of the INS in roll, pitch, and heading. By attaching an attitude monitoring system having the required resolution capability directly to the optical platform, improved positional accuracies can be achieved. This approach has been incorporated in the optical system concept.

3.1.2 Description of the Optical System Concept

The essential functional elements in the optical system are shown in figure 3-4, which is a schematic of the optical portion of the system. The optical path from the laser is transmitted to the scanning mirror, which directs the output beam downward to the surface of the water. The return beam from the water is deflected from the scanning mirror into the receiver and into a surface return detector as well.

The essential components in the optical system, and their respective functions are listed below:

a) Laser of appropriate power, wavelength, pulse repetition rate, etc., to be used as the light source for the hydrography measurements.

b) Output detector (beam monitor) to monitor the energy level of the laser and to provide timing synchronization.

c) Beam expander with adjustment for setting the divergence of the output beam to produce the desired spot size on the water.

d) Transmitter folding flat with adjustments for alining the output beam to the receiver axis.

e) Receiver telescope of adequate collecting aperture and a compact, folded, optical path.

f) Field lens to direct all of the collected signal into the collimating lens.

g) Field stop with provision for varying field of view to optimize signal to noise.

h) Spatial filter to obstruct the intense surface return from the receiver with provisions for varying the size of the obstruction.

i) Collimating lens to convert the divergent beam emanating from the field stop into a more nearly parallel beam to be transmitted by the narrow-band interference filter.

j) Spectral filter to suppress the background by blocking all wavelengths except that of the laser(with provisions for temperature control).

k) Re-imaging lens to concentrate the energy transmitted by the filter onto the face of the bottom return detector.

l) Neutral density filter for measured attenuation of collected energy during radiometric calibration of the receiver.

m) Bottom return detector, a gated photomultiplier to measure subsurface signals.

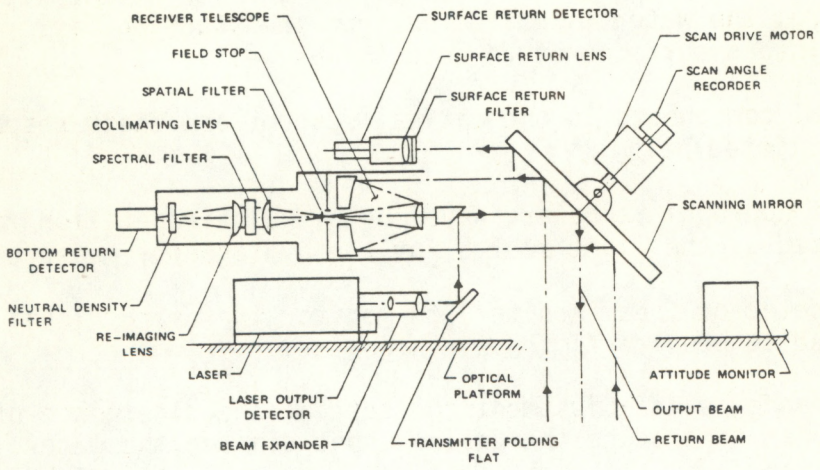

Figure 3-4. NOS hydrography system - optical system concept.

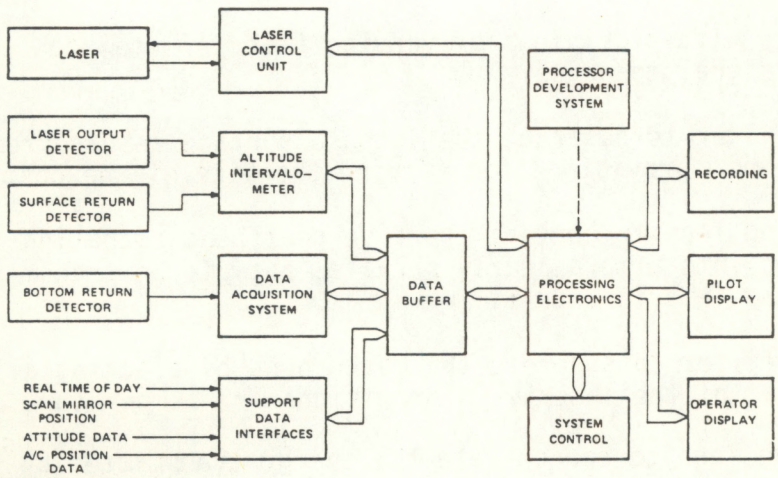

Figure 3-5. NOS hydrography system - electronics system concept.

n) Surface return detector consisting of a separate photomultiplier and collecting optics to collect the surface return and provide a reference pulse for gating the bottom return detector.

o) Optical platform to maintain optical alinement among the various components while isolating them from aircraft vibrations and shock.

p) Scanner consisting of a rotating optical flat with motor drive and means for monitoring the angular position of the scanning mirror.

q) Attitude monitor to measure changes in platform attitude caused by aircraft motion and to provide the reference axes for angular positioning of the output beam optical path.

3.2 Electronics System Concept

3.2.1 Concept Development

The electronics systems concept was developed based on an analysis of the NOS Hydrography System requirements and an evaluation of the performance of the AOL System. Improvements in the approach taken with the AOL System were incorporated as a result of the experience gained with the latter and advancements in the maturity of commercially available high-speed data acquisition and processing devices. Another major consideration was that of minimizing system weight, volume, and power requirements while selecting elements which would exhibit the desired performance. Data compression techniques were also considered which would significantly increase recording endurance without sacrificing system accuracy. In addition, emphasis was placed on the implementation of a dedicated processing system for the measurement application. With this in mind, the possibility of using a microprocessor or "computer on a board" was assessed and will be discussed. With this approach, it is envisioned that software changes would be generated on the ground using a software development system and then loaded into the hydrography system processor using magnetic tape as the transfer mechanism. A preliminary investigation of aircraft position fixing systems was conducted so as to be able to realize an accurate survey in the mapping process. Special attention was also given to the selection of a bottom return detector for the application which would provide the proper spectral response, sensitivity, gain, and ruggedness and have the capability for fast and controllable gating to attenuate the surface return signal level and reduce background effects.

The most dramatic change relative to the AOL System is in the approach used in the acquisition and processing of bottom signal returns. In the AOL System, a combination of nuclear and Camac devices was employed for return signal temporal gating and acquisition. Although utilized successfully, some problems were encountered using this approach. Briefly, the devices were limited in bandwidth, reflection coefficients were higher than desired at some of the connector fanout interfaces, and the dynamic range of the acquisition electronics (charge digitizers) was limited to $\sim$300:1 at the 2.5-nsec gatewidth required for the desired temporal resolution of the system, thereby introducing surface return

signal saturation effects. Because of this, the data collection and processing concept addressed these shortcomings and resulted in an approach which would eliminate these effects in the NOS Hydrography System.

3.2.2 Description of the Electronics System Concept

Figure 3-5 shows the basic electronics elements which are necessary to satisfy the NOS Hydrography System requirements. As is shown, an interface is necessary to control the laser and accept status information. The altitude intervalometer, which includes a laser output detector, surface return detector, and trigger, counting, and output logic, measures the distance between the system's exit aperture and the water surface. This data is required as an input for determining the geographic location of a data point. A gated bottom return detector and data acquisition system acquire and process the raw data necessary to determine water depth on a pulse-to-pulse basis. Several interfaces for data processing support purposes are required. These include real time of day (absolute time), scan mirror position, attitude data and aircraft position information. A data buffer is included to momentarily store a complete data set prior to processing. The processing electronics performs several real-time functions: system control, formatting for digital recording, real-time data assessment, formatting for graphics display purposes, navigational mapping, required aircraft course calculations, and status. System control is provided by a keyboard to input functional variables and control commands. A recorder provides a mission data tape compatible with ground-based data processing and reduction facilities. It would also be used to load programs and mission grid maps generated by a ground-based processor development system. The pilot and operator displays present identical data to aid the pilot in maintaining course and the operator in assessing system performance. The processor development system would be used to develop system software, as a system diagnostic tool, as a planning device for generating grid coordinate maps for each hydrography flight, and, possibly, as a "quick-look" data processing device.

4. PERFORMANCE CALCULATIONS

4.1 Introduction

This section contains calculations related to radiometric system performance, eye safety, and horizontal measurement accuracy.

4.2 Radiometric System Performance

4.2.1 Signal to Noise

The amplitude signal to noise, S/N_{AMP}, for the NOS Hydrography System can be determined on a single pulse basis from the relationship,

$$S/N_{AMP} = \frac{\phi_{DS}}{[\phi_{DS} + 2\phi_{DB} + 2\phi_{DWB} + 2\phi_{DA}]^{1/2}} , \quad (1)$$

where

ϕ_{DS} = detected signal count

ϕ_{DB} = detected upwelling background count from the ocean surface

ϕ_{DWB} = detected water backscatter count

and

ϕ_{DA} = detected background count from atmospheric scattering.

Here,

$$\phi_{DS} = \frac{Q}{h\nu} \frac{T_R T_{AW}^2 E_T \rho_B A_R e^{\frac{-2\beta H}{\cos\theta}} e^{\frac{-2kD}{\sqrt{1 - 9/16 \sin^2\theta}}}}{\pi(D + nH)^2} \quad (2)$$

$$\phi_{DB} = \frac{Q}{h\nu} T_R \Delta T_{GATE} N_\lambda A_R \Delta_\lambda \frac{A_{WR} \cos^2\theta}{H^2} e^{\frac{-\beta H}{\cos\theta}} \quad (3)$$

$$\phi_{DA} = \frac{Q}{4h\nu} T_R \Delta T_{GATE} H_\lambda A_R \Delta\lambda \Omega \cos^2\theta \frac{\beta'_{180}}{4\beta} (1 - e^{\frac{-\beta H}{\cos\theta}}) \quad (4)$$

and

$$\phi_{DWB} = \kappa \phi_{DS} = 2 \times 10^{-2} \phi_{DS} \text{ for } \Delta T_{GATE} = 2.5 \times 10^{-9} \text{ sec} . \quad (5)$$

The terms in equations (2) through (5) are as defined in table 4-1.

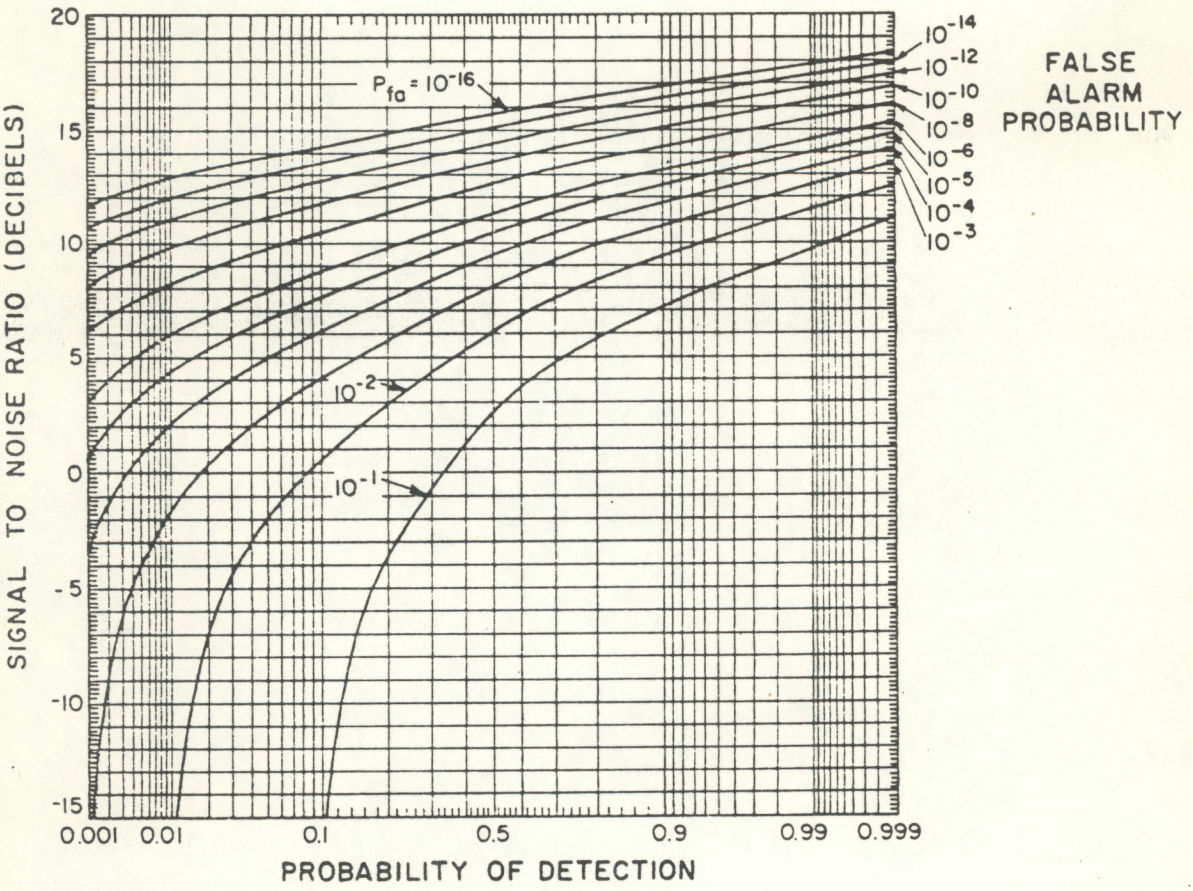

Figure 4-1. Signal-to-noise vs. detection and false alarm probabilities.

Using the values in table 4-1, at a typical operating altitude of 304 m, the following signal levels are calculated from equations (2) through (5):

$\phi_{DS} = 9.26 \times 10^2$ photoelectrons (pe)

$\phi_{DB} = 4.03 \times 10^2$ pe

$\phi_{DA} = 1 \times 10^2$ pe

$\phi_{DWB} = 1.85 \times 10^1$ pe

Using equation (1), the signal to noise, $S/N_{AMP} = 20.8$ and the power signal-to-noise, $S/N_D = 432$. Using the well-known relationship from radar technology[7] between power signal to noise, false alarm probability and probability of detection, shown in figure 4-1, yields for this case a probability of detection, $P_D > 0.999$ and a false alarm probability, $P_{FA} < 10^{-25}$, both far in excess of that required to assure good system performance as specified in table 2-2. If the aircraft altitude is increased to the maximum desired, 914 m, and the receiver field of view is reduced to a value estimated to be optimum for that altitute, 18 mr, with a corresponding reduction in A_{WR} and Ω, then $S/N_{AMP} = 4.46$ (19.9 power). This yields a $P_D = 0.95$ and a $P_{FA} \leq 10^{-5}$ indicating that, for the conditions chosen, high altitude mapping operations will best be performed at night.

4.3 Eye Safety Considerations

The emission limit for a scanning Class I laser system operating between 400 and 700 nm is 5×10^{-7} J/cm^2 (single pulse) (ref. 8). This is the radiant exposure allowed to fall on the cornea of a dark adapted eye (7 mm dia.) at night. The beam divergence, Θ_d, necessary to satisfy this requirement can be determined from the relationship.

$$\Theta_d = \frac{\left[\frac{4E_T e^{-\beta H}}{5 \times 10^{-7} \pi}\right]^{1/2}}{H} , \qquad (6)$$

where all terms are as defined in table 4-1. Therefore, for a 1 mJ laser pulse energy, the beam divergence required at the lowest expected operating altitude of 152 m is 3.3 mr. At the nominal operating altitude of 304 m, a beam divergence of 1.62 mr would be required to satisfy the Class I emission limit. Since mapping operations will probably be conducted with beam divergences in excess of $\sim$4 mr for laser-water interface optimization, no constraints in system operation are envisioned as a result of eye safety limitations.

Table 4-1. Assumed system, atmospheric and oceanographic parameters

Symbol	Definition	Value
Q	Detector Quantum Efficiency	0.1 pe/phot
$h\nu$	Photon Energy	3.6×10^{-19} J/phot (532 nm)
T_R	Receiver Transmission	0.3
T_{AW}	Air-Water Interface Transmission	0.98
E_T	Transmitted Laser Pulse Energy	10^{-3} J
ρ_B	Bottom Reflectance	0.15
A_R	Receiver Area	3.24×10^{-2} m^2 (8" dia)
β	Air Path Attenuation Coefficient	1.2×10^{-4} m^{-1} (clear air)
β'_{180}	Air Volume Backscatter Coefficient	4.5×10^{-5} m^{-1}
θ	Scan Angle From Nadir	15^o
k	Water Path Attenuation Coefficient	1.06×10^{-1} m^{-1} (see Section 2.0)
D	Bottom Depth	30 m
n	Sea Water Index of Refraction	1.33
H	Aircraft Altitude	304 m
ΔT_{GATE}	Receiver Time Gate	2.5×10^{-9} sec
N_λ	Daylight Water Radiance	2×10^{-2} Wm^{-2} $ster^{-1}$ nm^{-1}
H_λ	Sun Spectral Radiance	1.38 Wm^{-2} $ster^{-1}$ nm^{-1}
$\Delta\lambda$	Receiver Optical Bandwidth	1.7 nm
A_{WR}	Receiver Area on Water Surface	182 m^2 (for a 50 mr FOV at 304 m)
Ω	Receiver Solid Angle	1.9×10^{-3} ster (50 mr FOV)
κ	Water Backscatter/Signal Ratio	2×10^{-2} (for ΔT_{GATE} = 2.5×10^{-9} sec)

4.4 Horizontal Absolute Position Measurement Uncertainty

An estimate was made of the expected absolute horizontal position uncertainty of an NOS Hydrography System bathymetry measurement. The total horizontal position measurement uncertainty, σ_R, can be determined from the relationship,

$$\sigma_R = \left[\sigma_p^2 + \sigma^2_{rh_x} + \sigma^2_{rh_y} + \sigma^2_{\theta_s} + \sigma^2_d + \sigma^2_{pr} + \sigma^2_{pp} + \sigma^2_{py} + \sigma^2_f \right]^{1/2}, \quad (7)$$

where (for an aircraft altitude of 304 m and scan angle of 15°)

σ_p = aircraft horizontal position uncertainty

σ_{rh_x} = resultant of roll, pitch, and heading uncertainties perpendicular to the aircraft roll axis

σ_{rh_y} = resultant of roll, pitch, and heading uncertainties along the aircraft roll axis

$\sigma\theta_s$ = scan encoder readout uncertainty = 5.27 min (12 bit) = 0.48 m rms

σ_d = scan encoder digitization error = 0.02° = 0.1 m rms

σ_{pr}, σ_{pp}, σ_{py} and = optical platform component alinement error and platform misalinement with datum in the roll, pitch, and yaw axes, respectively ($\sigma_{pr} = \sigma_{pp} = 0.3$ mr = 0.09 m rms; $\sigma_{py} = 0.35$ mr = 0.11 m rms)

σ_f = measurement uncertainty due to aircraft flexure = 0 since the attitude measurement unit is assumed mounted on the optical platform.

The resultant of roll, pitch, and heading uncertainties perpendicular to and along the aircraft roll axes, σ_{rh_x} and σ_{rh_y} respectively, can be determined from the expressions,

$$\sigma_{rh_y} = \left[\sigma^2_{r_s} \sin^2\theta \sin^2\theta_h + r_v^2 (\sigma^2_{\theta_r} + \sigma^2_{\theta_s}) + r^2_s \sin^2\theta \sin^2\theta_h \sigma^2_{\theta_h} \right]^{1/2} \quad (8)$$

and

$$\sigma_{rh_y} = \left[\sigma^2_{r_s} \sin^2\theta \cos^2\theta_h + r_v^2 (\sigma^2_{\theta_p} + \sigma^2_{\theta_s}) + r^2_s \sin^2\theta \cos^2\theta_h \sigma^2_{\theta_h} \right]^{1/2}, \quad (9)$$

where

σ_{rs} = measurement uncertainty along the laser line of sight = 0.3 m rms

Θ = effective scan angle = $\Theta_s \pm \Theta_{r,p}$

Θ_h = disturbance angle in heading = 1.0^o

r_v = aircraft altitude = 304 m

$\sigma_{\Theta r}$ = measurement uncertainty in aircraft roll = $0.2^o = 3.5 \times 10^{-3}$ rad rms

$\sigma_{\Theta s}$ = as defined above

r_s = distance from the aircraft to the water surface along the laser line of sight

$\sigma_{\Theta h}$ = measurement uncertainty in aircraft heading = $1.0^o = 1.75 \times 10^{-2}$ rad rms

and

$\sigma_{\Theta p}$ = measurement uncertainty in aircraft pitch = $0.2^o = 3.5 \times 10^{-3}$ rad rms.

From equations (8) and (9) and for a scan angle Θ_s of 15^o and an aircraft altitude of 304 m, σ_{rh_x} = 1.52 m rms and σ_{rh_y} = 1.43 m rms. Combining uncertainties in equation (7) yields:

$$\sigma_R = \left[\sigma_p^2 + 4.6\right]^{1/2} \text{ m.} \qquad (10)$$

Using the measured accuracy of the Cubic Corp. Autotape system of σ_p=4.6 m rms from ref. 9, σ_R = 5.0 m rms. (See also section 5.3.1.10.) Thus, at an aircraft altitude of 304 m or less, the projected absolute horizontal bathymetry measurement accuracy of the NOS Laser Hydrography System meets the 1:5,000 chart survey scale positional accuracy requirement of 5 m, 1σ.

5. LIMITED SYSTEM DESIGN

5.1 Introduction

In this section, the limited design of the NOS Hydrography System is developed.

5.2 Optical System

5.2.1 Description of Optical System Elements

5.2.1.1 Optical Platform

Figure 5-1 is a layout of the recommended optical configuration showing the transmitter, receiver, scanner, and attitude monitor all mounted to a common platform. The platform serves as an optical bench to hold the optical components in precise alinement to one another and, through passive isolators, provides a means of isolating the units from aircraft shock and vibrations, an important consideration for maintaining stability and assuring long operating life. The second function of the platform is to provide a convenient means of installing and removing the assembly from the aircraft. To keep the overall length of a reasonable value of ~60", the receiver telescope utilizes folded optics, and a folding flat is provided in the optical path leading to the bottom return detector. Further reduction of the overall length is limited by the large scanner assembly and by the long focal length of the collimating lens which will be discussed later in connection with the interference filter. The 28" width of the platform will accommodate the scanner assembly and the laser, which is placed along one side of the receiving optics; the surface return detector, its optics, and the attitude monitor are shown beside the receiving optics on the opposite side of the platform.

Figure 5-2 is a layout of the NOS Hydrography System in the Beechcraft King Air, the smaller candidate aircraft considered. This aircraft is assumed to have been previously modified to accommodate aerial cameras pointed downward through two optical windows in the underside of the aircraft. By removing the cameras from the window stations, the laser Hydrography System can be interchanged with the camera system as required. Simple crossbars would be used to interface the platform with the seat rails on the aircraft floor with passive isolators located at the interface. Removal of the platform would involve the removal of a fastener at each isolator. This concept places a constraint on the size of the optical assembly to assure a fit with the aircraft windows, floor rails, airframe, and doorway. Figure 5-2 depicts the most reasonable fit of the optical assembly at the forward window, with adequate clearances to the airframe and adequate access to the optical components for adjustment and operation. Passageways are also adequate for reaching the pilot's compartment and for removing the unit through the aircraft door. During removal, it is expected that the scanner would be detached from the platform to lighten the load, and the platform, with the optics attached, would be turned on its side to pass through the doorway. A cutaway view of the King Air is shown in figure 5-3, with the major system components identified.

The second aircraft considered was the DeHaviland Buffalo which is considerably larger than the King Air. It is expected that the recommended configuration would fit in either aircraft. Very few system-related advantages can be identified which would offset the higher operating cost of the larger aircraft. It is possible that the larger aircraft would enable a more permanent installation to be used, but the portability of the recommended configuration and the simplicity of detaching the platform from the isolators made a permanent installation only a minor advantage on the larger aircraft.

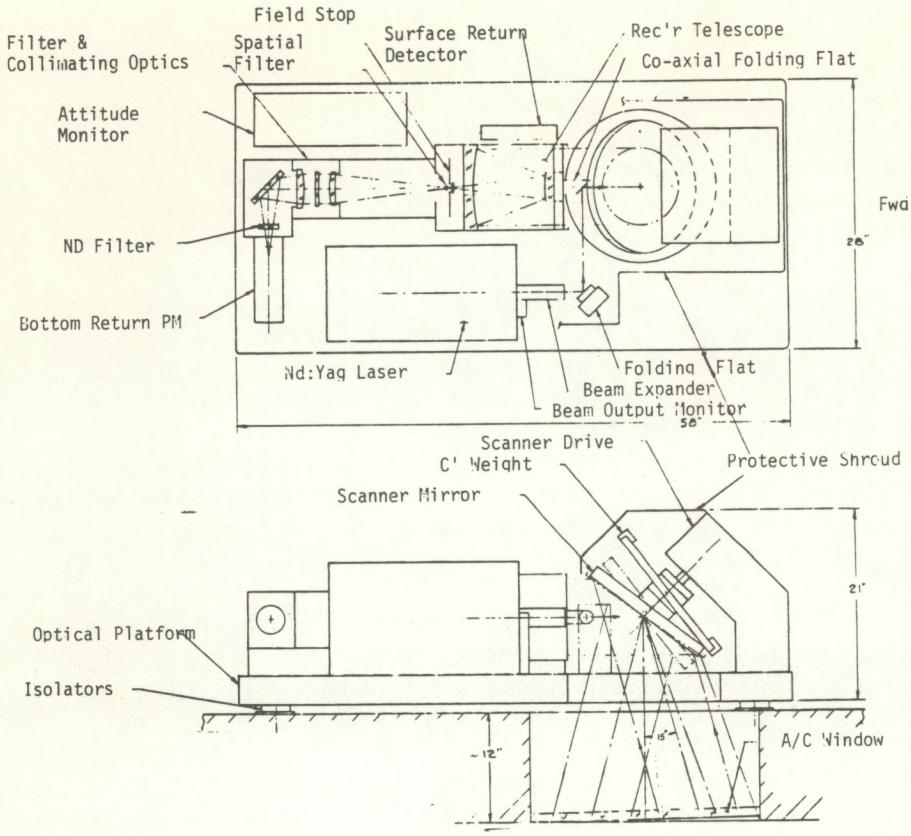

Figure 5-1. Optical system layout.

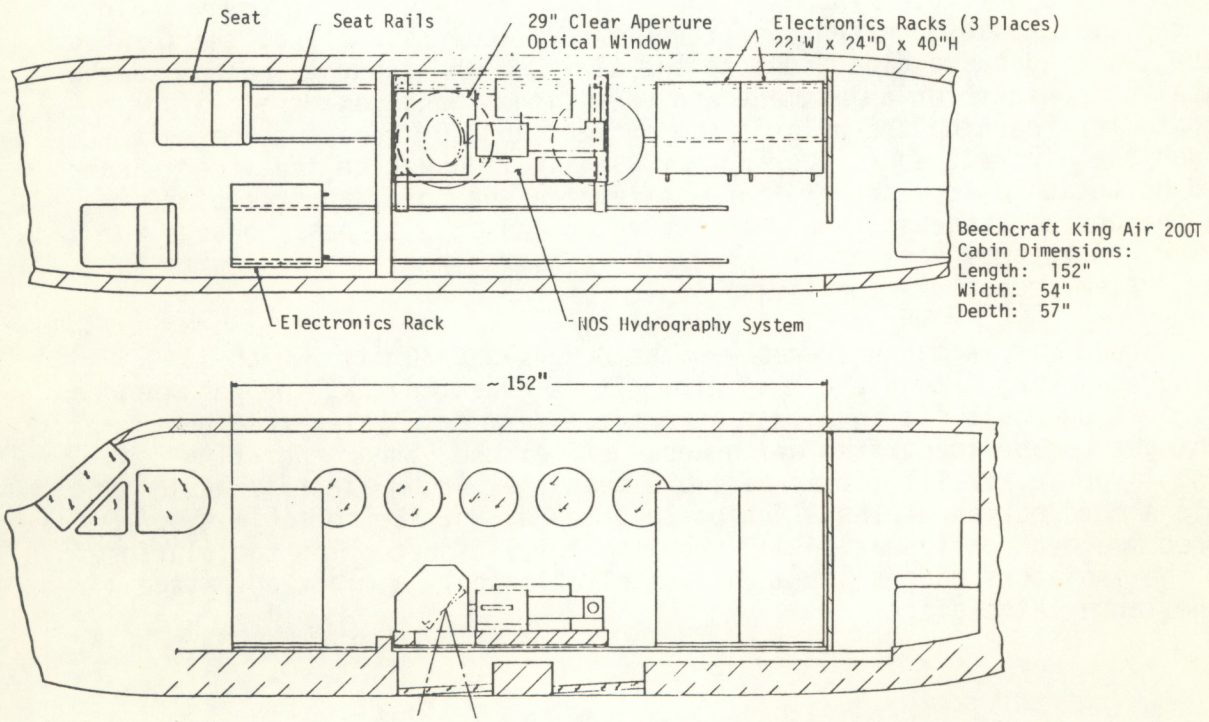

Figure 5-2. Equipment layout in Beechcraft King Air.

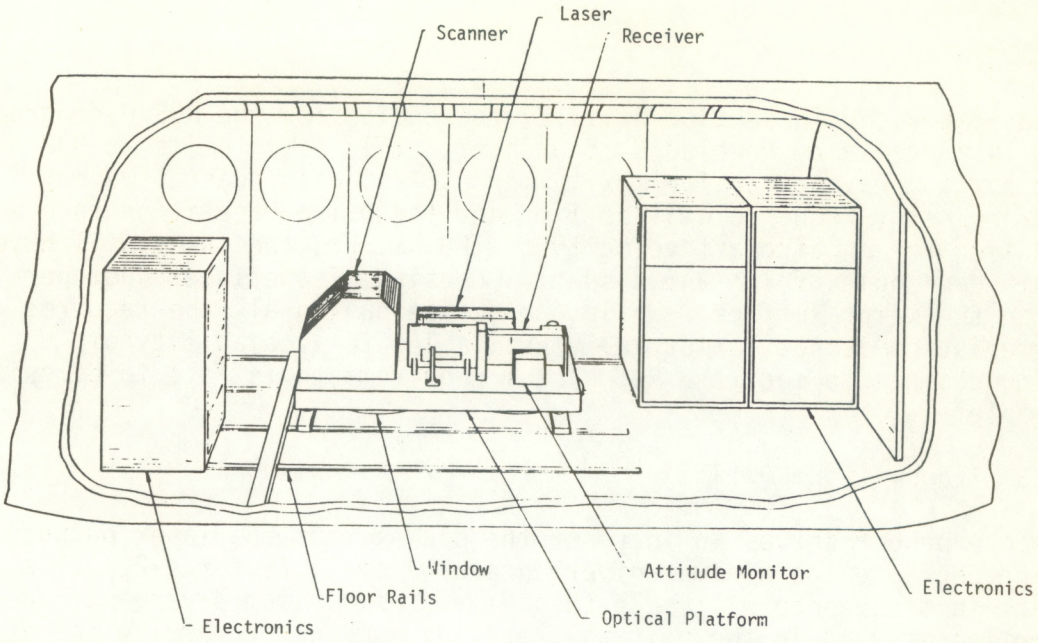

Figure 5-3. Cutaway view of Beechcraft King Air.

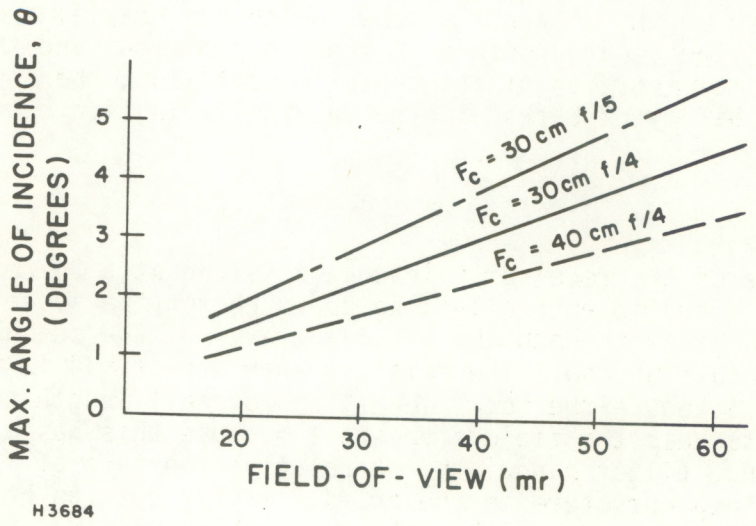

Figure 5-4. Factors affecting angle of incidence.

5.2.1.2 Laser

As was discussed in section 3.1.1.2, the choice for the NOS Hydrography System is a frequency doubled Nd:YAG laser. This laser emits at 532 nm, a near optimum wavelength for maximum transmission in coastal waters. The laser energy required will be 1 mJ and the pulse repetition rate $\geq$ 500 Hz. As required for an aircraft velocity of 120 nmi/hr, the laser will have a maximum scan angle of 15^{o} and a spatial density of one laser spot per 20 m^2 on the water surface. While the device having all the required characteristics is not commercially available, the scalability of existing designs to meet the NOS system requirements is felt to be quite achievable.

5.2.1.3 Transmitting Optics

A beam expander serves to increase the diameter of the laser output beam and decrease the minimum divergence by a small factor, ~2. This decrease in divergence will help to achieve the minimum divergence desired, and the lenses used in the unit will provide a means of varying the divergence for different missions. A range of beam divergence settings from 2.5 to 50 mr is readily achieved with a 2X beam expander.

An adjustable folding flat deflects the beam from the expander over to the scanning mirror. In figure 5-1 the beam is directed to the center of the scanning mirror by means of a coaxial folding flat placed within the center obscuration of the Cassegrain telescope. An alternate arrangement would be to place a second folding flat on the near side, external to the telescope aperture, so that the output beam is deflected to the unused margin of the scanning mirror. This, however, would require a slightly larger clear aperture at the aircraft window. With the coaxial arrangement shown in the figure, the clear aperture is kept to a minimum and the output beam fits within a small portion of the center obscuration, thereby minimizing the possibility of backscattered laser illumination reaching the receiver optics.

5.2.1.4 Telescope

The clear aperture of the receiver telescope is sized at a 20-cm (8") diameter to provide a sufficient collecting aperture for the system and to provide a reasonable fit with both the angular travel of the scanner and the size of the aircraft window. The relative aperture of f/4 is made as small as practical to reduce the focal length and overall length of the telescope and also to keep the field stop small because this has a direct effect on interference filter bandwidth. A relative aperture of f/4 requires a fairly steep curvature in the primary mirror but can be manufactured with careful hand polishing to a suitable quality for the degree of resolution required.

The choice of f no. also affects the collimating lens diameter and consequently the filter diameter. These topics will be covered in a later section.

The recommended telescope design shown in the figure is Cassegrainian. This configuration was chosen because of its compact size and minimum number of optical surfaces. During detailed design, it would be determined whether the telescope should be locked at a fixed separation from the field stop, based on an intermediate object distance, or contain focus adjustments for use over the specified altitude range. (Adjustments of the collimating optics could also be investigated in this regard.)

The center obscuration of the telescope would be ~3.5" dia. to provide proper baffling with the large field of view desired. The center obscuration could be designed to allow a small fraction of the laser output to be scattered into the receiver optics during system calibration for radiometric response measurements.

5.2.1.5 Field Stop and Spatial Filter

The field stop establishes the instantaneous field of view of the receiver. A range of settings would be available by the provision of a continuously adjustable field stop. The largest setting would be 1.6" in diameter to provide a 50 mr field of view. With this field of view, it would be necessary to include a field lens located very close to the field stop for the purpose of imaging the collecting aperture of the telescope onto the collimating lens, thereby preventing vignetting of off-axis image points.

The recommended design also includes a spatial filter or center mask located very close to the field stop for the purpose of obscuring the central portion of the field of view. This obscuration will help prevent the strong reflection from the illuminated surface of the water from being reflected into the receiver and saturating the bottom return detector. The size and quantity of spatial filter obscurations will be finalized during detailed system design but will probably vary from 0 to 6 mr and be approximately six in number.

5.2.1.6 Interference Filter and Collimating Optics

The function of the interference filter in the receiver is to transmit the signal at the laser wavelength and to reject background energy at the adjacent wavelengths within the bandpass of the photomultiplier tube. The desired characteristics are maximum transmission at the laser wavelength and minimum bandwidth for signal-to-background optimization. However, to be practical, the bandwidth should be large enough to accommodate detuning of the filter caused by such factors as ambient temperature variations, manufacturing tolerances, and variations in angle of incidence.

The angle of incidence is a function of the receiver field of view and the focal lengths of the collecting and collimating optics. Figure 5-4 shows the maximum angle of incidence for different size collimating optics used with collectors of different f nos. In the recommended design, an overall layout was developed which fits into the King Air aircraft and provides a space allocation for an f/4 collecting telescope and a collimating lens of 30-cm (12") focal length. If we assume these values to be fixed, we can proceed to compare filters of various bandwidths and also examine the effect of receiver field of view on filter transmission.

Figure 5-5 shows the peak wavelength shift with varying angle of incidence for an interference filter. Also shown is the field of view which corresponds to the maximum angle of incidence for the plotted values. The figure shows that, with the 30-cm focal length collimating optics, a 50-mr field of view encompasses angles of incidence up to 3.8^{o} with an attendant maximum wavelength shift of 0.57 nm.

The effect of wavelength shift on filter transmission is shown in figure 5-6 which is a transmission curve for a typical two-period filter such as that considered for use here. The transmission values shown are relative to the peak transmission and can be expected to be in the vicinity of 60 percent for a half-peak bandwidth (HPBW) of over 0.8 nm. Good transmission is assured by confining the wavelength shift to the region of the curve above the 80 percent relative transmission level, which coincides with 0.33 HPBW on the wavelength scale. If we allow the maximum wavelength shift of 0.57 nm established above, the required HPBW = 5.7/0.33 or 1.7 nm. This is a wider filter bandpass than the 0.4 nm filter used in the AOL System because of the larger field of view required and the shorter collimator focal length selected here.

The effect of wavelength shift on filter transmission is shown in figure 5-7, where filters of different HPBW are compared at various angles of incidence. The transmission relative to peak is shown at the left. The scale at the right shows the resulting transmission when a peak value of 60 percent is assumed. A second scale at the bottom of the figure indicates the field of view which encompasses a maximum angle of incidence corresponding to the plotted values. For the 1.7-nm filter suggested in the previous paragraph, the transmission would be about 47 percent. This is a conservative estimate based on a wavelength shift associated with the maximum angle of incidence. A more accurate estimate would require integration over all angles of incidence from zero to the maximum with consideration for the energy distribution of the signal within the receiver field of view. It can also be seen from the figure that angles of incidence less than 1.5^{o} (20-mr field of view) will suffer no loss in transmission from the maximum.

Using a bandpass of 1.7 nm, we now examine the effect of temperature variations on wavelength shift. Vendor estimates on temperature sensitivity vary from 0.016 to 0.03 nm/^{o}C, and experience with the AOL System indicates that the ambient temperature in the aircraft can rise as high as 20^{o}C above normal laboratory conditions. If we assume $\pm$ 10^{o}C variation from an elevated operating point, the wavelength shift resulting from the temperature

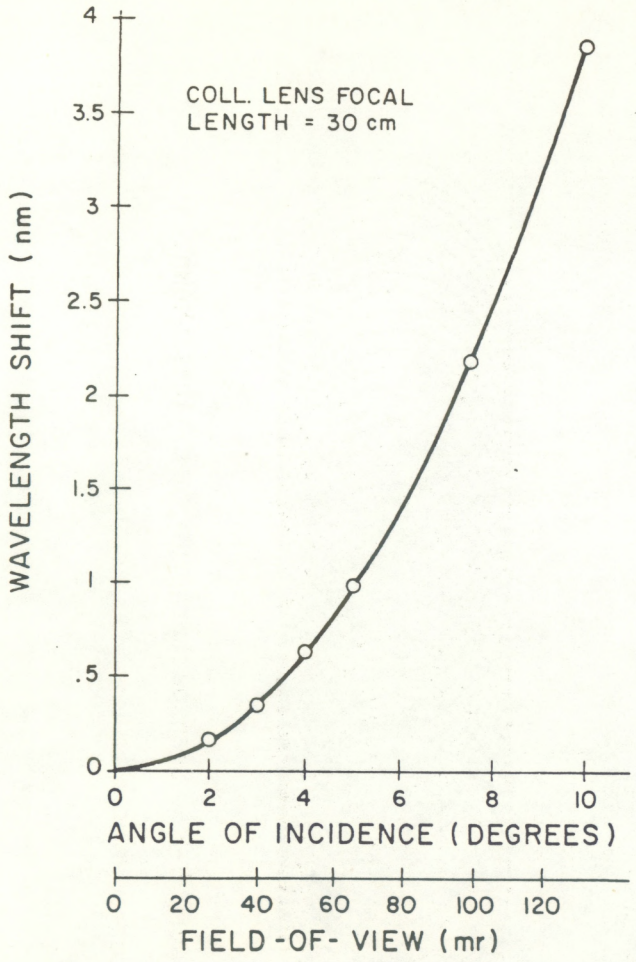

Figure 5-5. Wavelength shift due to angle of incidence.

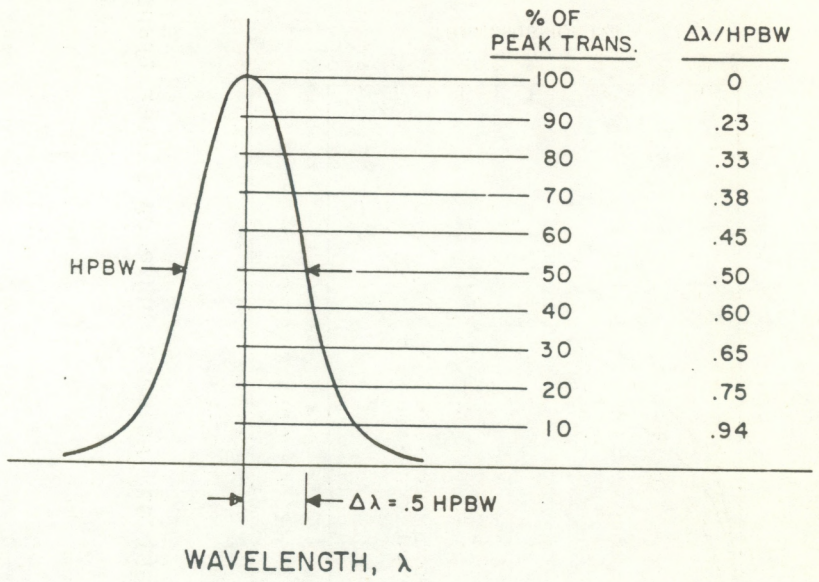

Figure 5-6. Spectral transmission of interference filter.

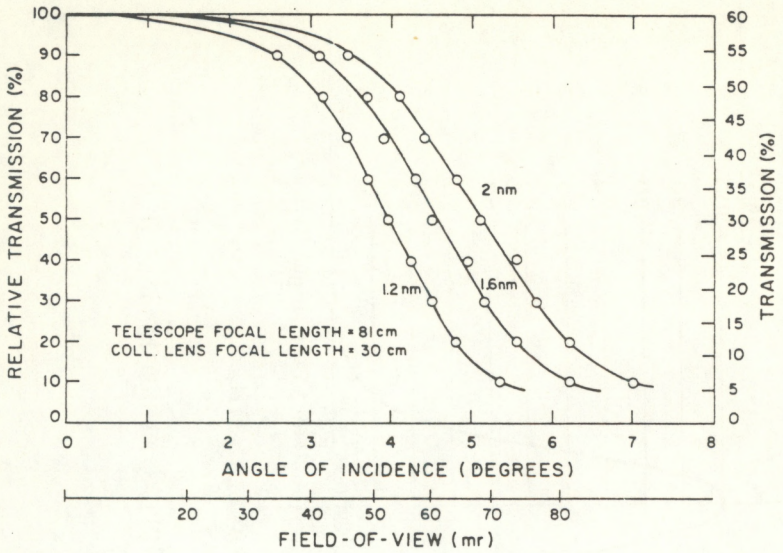

Figure 5-7. Effect of incident angle on filter transmission.

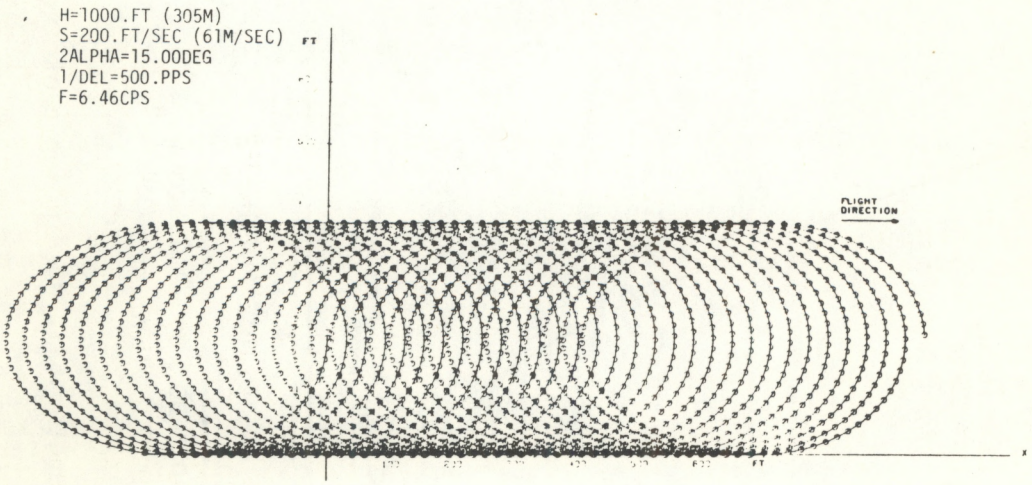

Figure 5-8. Scan pattern for conditions shown.

variation would be 0.15 to 0.3 nm. This is rather small when compared with the 1.7-nm bandpass of the filter. However, a significant improvement is possible by utilizing a thermostatically controlled heater blanket around the filter housing. Vendor estimates indicate that the temperature of the housing can be readily maintained to within $\pm$ 1°C of the selected operating point, resulting in a wavelength control of better than 0.03 nm.

A final consideration in regard to the filter specification is the manufacturing tolerance on peak wavelength. Vendor catalogs normally specify this tolerance at + 10 percent of HPBW which would result in a 0.017-nm error. However, custom filters are made to within 0.002 nm. Another technique for reducing this effect is to establish a tentative filter operating temperature which is a few degrees higher; then, after the filter is made, the operating temperature can be raised or lowered the precise amount necessary to tune the filter to its optimum operating wavelength.

5.2.1.7 Re-Imaging Lens and Neutral Density Filter

The return beam passes through the interference filter and is then reimaged onto the face of the bottom return photomultiplier. A single-element lens is suitable for reducing the beam diameter from 8.8 cm (3.5") down to less than 5 cm (2"). The front surface of the photomultiplier is placed forward of the image plane to provide a more uniform distribution of signal energy over the front of the tube. A neutral density filter is also provided just forward of the tube to be used during radiometric calibrations of the receiver. The filter should be conveniently removable for normal mission operation.

5.2.1.8 Surface Return Detector

The surface return detector consists of a separate photomultiplier and collecting optics to collect the surface return and provide a reference pulse for gating the bottom return photomultiplier. The need for a separate detector to collect the surface return is based on the large dynamic range of the return signal. By separating the return pulse into two time regimes, it is possible to reduce the dynamic range required in each region to a level which is more compatible with the signal processing electronics. To implement this concept, a surface return detector is required which is separate from the receiver and detects only the strong surface return signal. The bottom return photomultiplier tube is then gated on by the surface return detector to measure the reduced signal which follows the peak. To additionally attenuate the peak level in the receiver, a spatial filter is placed at the center of the field stop to block the central region where the surface return is concentrated. This filter was previously discussed in section 5.2.1.5.

5.2.1.9 Scanner

The essential elements of the scanner include a lightweight mirror approximately 15" in diameter which directs the output beam downward to the water and reflects the return beam over to the receiving optics. A drive motor rotates the mirror and causes the optical path to move across the water in an elliptical scan pattern, while an angle encoder monitors the angular position of the scanning drive at a suitable sampling rate. The scanning pattern is adjustable for normal or concentrated scanning patterns, and the scanning frequency is variable for optimizing laser spot separation on the water surface. The design is the same in principle as that used in the AOL System but, in the King Air aircraft, the unit would be alined with the longitudinal axis of the aircraft rather than the lateral axis. This orientation causes the major axis of each elliptical scan to be alined with the direction of aircraft motion as is shown in figure 5-8. The properties of this type of scanner are analyzed in ref. 6.

The scan pattern in figure 5-8 is chosen to produce a laser spot distribution of one spot for every 20 m^2 of water area with a spot rectangularity of 1.0. The rectangularity is based on the lateral separation of spots compared with the average longitudinal spacing near the center of the swath. At the outer edges of the swath, the lateral spacing becomes very close and provides a redundancy of measurements which is useful for diagnostic purposes.

Figure 5-9 shows the effect of increasing the scan frequency; the lateral spacing increases and the longitudinal spacing decreases, thereby providing an effective control of rectangularity.

Figure 5-10 shows a concentrated scan achieved by decreasing the aircraft altitude, setting the scan angle to 5^o, and increasing the scan frequency to 12 Hz. The reduced scan angle narrows the lateral spot spacing, and the net effect of the increased frequency is to narrow the longitudinal spacing. These figures indicate the controls that are available on the scanner for optimizing the scan pattern. Aircraft speed, laser repetition rate, and altitude also effect the scan pattern.

The scanner configuration described by figures 5-8 through 5-10 involves an important functional limitation in that if the mirror is set for $\pm 15^o$ coverage along the major axis of the ellipse, then the swath width, which is sized by the minor axis of the ellipse, becomes approximately 10.5^o. If this is not adequate coverage from an operational viewpoint, then another option would be to increase the scanning angle to the maximum value that the aircraft window will accommodate. A preliminary layout based on nominal dimensions of the King Air aircraft indicates that the scanning angle could be increased to $\pm 19^o$ in a forward-to-aft direction producing a scanning width of $\pm 13^o$. However, the increase in scanning angle also produces an increase in lateral spot separation, which means a reduction in area coverage per spot.

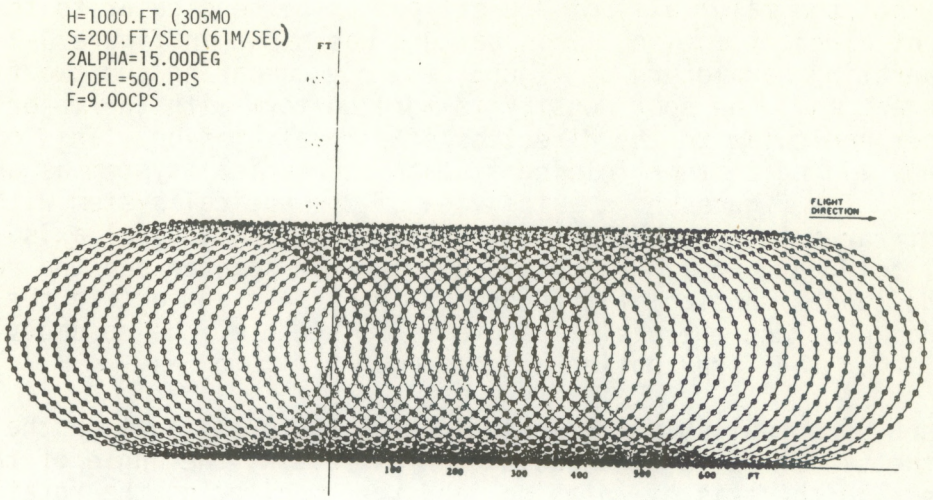

Figure 5-9. Scan pattern for conditions shown.

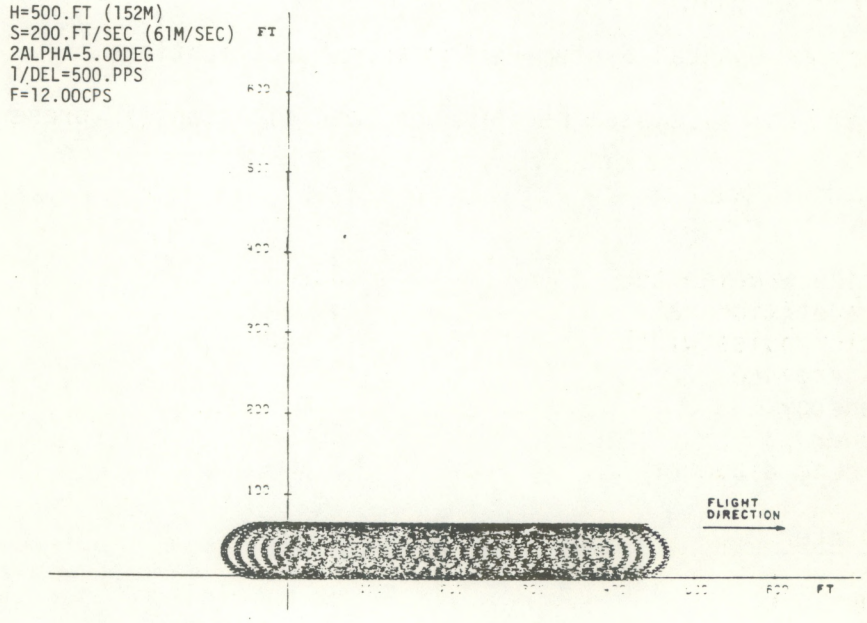

Figure 5-10. Concentrated scan pattern.

A more effective scanning pattern is achieved by orienting the scanning mirror so that the major axis of the ellipse is perpendicular to the direction of aircraft motion. This pattern was shown in figure 3-1 for similar operating parameters as figure 5-8. By comparing the two figures, it is apparent that the spot density is more uniform with the major axis oriented perpendicular to the direction of aircraft motion. This option is available by adding another folding flat to the optical system as shown in figure 5-11. The figure shows a top view of the optical system with the scanning mirror axis rotated 90^{o} to the aircraft longitudinal axis. The additional folding flat is introduced between the scanner and the receiver so that the long dimension of the assembly runs fore and aft in the aircraft and does not obstruct the aisle. The overall width of the assembly is slightly larger than the configuration shown in figure 5-1.

The method of establishing the pointing angles to the spot on the water involves the use of calibrated positions for setting the angle of the mirror with respect to the axis of rotation and then monitoring the rotation angle by means of an encoder which records the angle at suitable intervals. These angles are referenced to the attitude monitoring equipment on the optical platform.

5.2.1.10 Optical System Weight Estimates

The weight of the entire optical assembly including the platform and scanner is estimated to be 290 lb. (130 kg). The weight allocation by major subassembly is shown in table 5-1.

5.2.2 Summary of Optical System Performance Specifications

A summary of optical system performance specifications is presented below:

A. Laser

Excitation wavelength	532 nm
Pulse repetition rate	$\geq$ 500 Hz
Excitation pulse width	$\leq$ 5 nsec
Beam divergence	$\leq$ 5 mr
Pulse energy	1 mJ
Peak power	200 kW
Output beam diameter	3 mm

B. Beam expander

Exit aperture	20 mm minimum
Divergence range	2.5 - 10 mr
Magnification	2X

Table 5-1. Optical system weight estimates

Equipment Item/Module	Est. Weight (lb)
Nd:YAG Laser	55
Transmitting and Receiving Optics	35
Optical Platform	80
Scanner	100
Attitude Monitor	20
	290 (130 kg)

Table 5-2. Characteristics of FND-100 photodiode

Characteristic	Typical Value	Comments
Wavelength	300 - 1,100 nm	
Bandwidth	350 MHz	
Responsivity	0.62 A/W	At 900 nm
Risetime	< 1 nsec	At 50 Ω
Dark Current	< 100 namp	
Noise Current	1.8×10^{-13} A/Hz$^{1/2}$	At 1 kHz
Linearity	± 2%	Over 7 decades

Table 5-3. Characteristics of the RCA 8644 photomultiplier

Characteristic	Typical Value
Quantum Efficiency at 532 nm	10%
Gain	7×10^5 at 2000 V
Dark Noise	3×10^{-9} at 30 A/lm
Maximum Anode Current	0.1 mA average
Anode Risetime	1.5 nsec
Diameter	1.9 cm
Length	9.65 cm

Table 5-4. Characteristics of the ITT F4084 photomultiplier

Characteristic	Typical Value
Quantum Efficiency at 532 nm	11%
Grid (100 lines/in.)	80% transmission (optical)
Number of Dynodes	8
Risetime	1.5 nsec
Current Amplification Maximum	10^6
Average Anode Current Maximum	2 mA average
Peak Anode Current Maximum	200 mA
Grid Cutoff	-2 V
Grid Gating Time	< 5 nsec
Gain Control	4 to 5 decades
Typical Grid Gating Characteristics	See Fig. 5-13

C. Transmitter folding flats

Adjustable flat	~30 mm diameter with two-axis adjustment for alinement
Folding flat	~75 mm x 50 mm at 45°

D. Telescope

Entrance aperture	200 mm diameter (8")
Relative aperture	f/4
Center obscuration	~89 mm (3.5")
Field of view	50 mr maximum

E. Field stop assembly

Size	Variable up to 40 mm (1.6") diameter to accommodate 50 mr field of view
Spatial filter	Variable mask to obscure center portion of field stop (obscuration range 0 to 6 mr, to be finalized during detailed system design)
Field lens	40 mm clear aperture lens to image entrance aperture onto collimating lens aperture

F. Collimating lens

Focal length	305 mm (12")
Relative aperture	f/4

G. Spectral filter

Bandwidth	~2 nm HPBW
Center wavelength	532 nm
Transmission at center wavelength	60% minimum
Size	90 mm (3.5") diameter
Temperature control	Maintainable to $\pm$ 1°C of operating point

H. Re-imaging lens and ND filter

Focal length	270 mm (10.6")
Relative aperture	f/3
Image size	36 cm (1.4") diameter
ND filter	60 mm diameter removable

I. Surface return detector optics

Collecting lens	~25 mm (1") diameter, f/4
Filter	~3 nm HPBW with peak wavelength at 532 nm
Field of view	~10 mr

J. Scanner

Type	Rotating mirror scanner
Mirror size	38 cm (15") diameter
Scanning angle	$\pm$ 15° from nadir with adjustments for $\pm$ 10°, $\pm$ 5°, and zero degrees
Scanning frequency	Adjustable from 5-12 Hz
Output encoder accuracy	$\leq$ 5.27 min

5.3 Electronics System

5.3.1 Description of Electronics System Elements

Figure 5-12 is a block diagram of the electronics system and indicates the major functions and subsystems required to satisfy this application. Each of the system elements and overall processing functions are described in the following paragraphs.

5.3.1.1 Altitude Intervalometer

An integrated approach would be used to implement the altitude intervalometer to provide a digital readout directly in meters. This would unburden the real-time processing requirements in that time-to-distance conversions would not have to be made by the latter and would also reduce the size and weight required for this function. The unit would be capable of measuring distances from 100 to 1000 m to $\pm$ 0.3 m accuracy.

The approach to be implemented would use a "coarse" counting and "fine" Wilkinson Integrator time-to-digital conversion technique. A counter would be enabled by the laser output detector and would count a calibrated clock sequence such that each count would be equivalent to 10 m. Since the clock would be asynchronous with "count enable," the time offset must also be measured to maintain the desired accuracy. This would be accomplished using a Wilkinson Integrator having an intrinsic resolution of $\pm$ 200 psec, which is more than adequate to preserve the required intervalometer accuracy of $\pm$ 0.3 m. When a surface return is detected, the counter would be stopped and would contain the distance to a 10 m resolution. The surface return is also asynchronous with the clock edge and would also be measured using a second Wilkinson Integrator. An integral hardwired arithmetic unit would process and account for the asynchronism to provide an output directly in meters to the required accuracy and resolution.

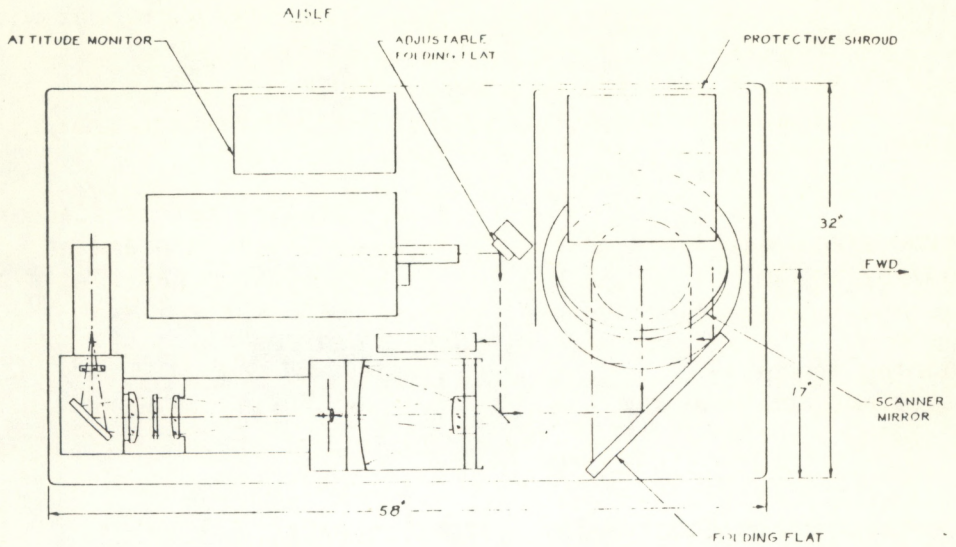

Figure 5-11. Alternate optical system layout.

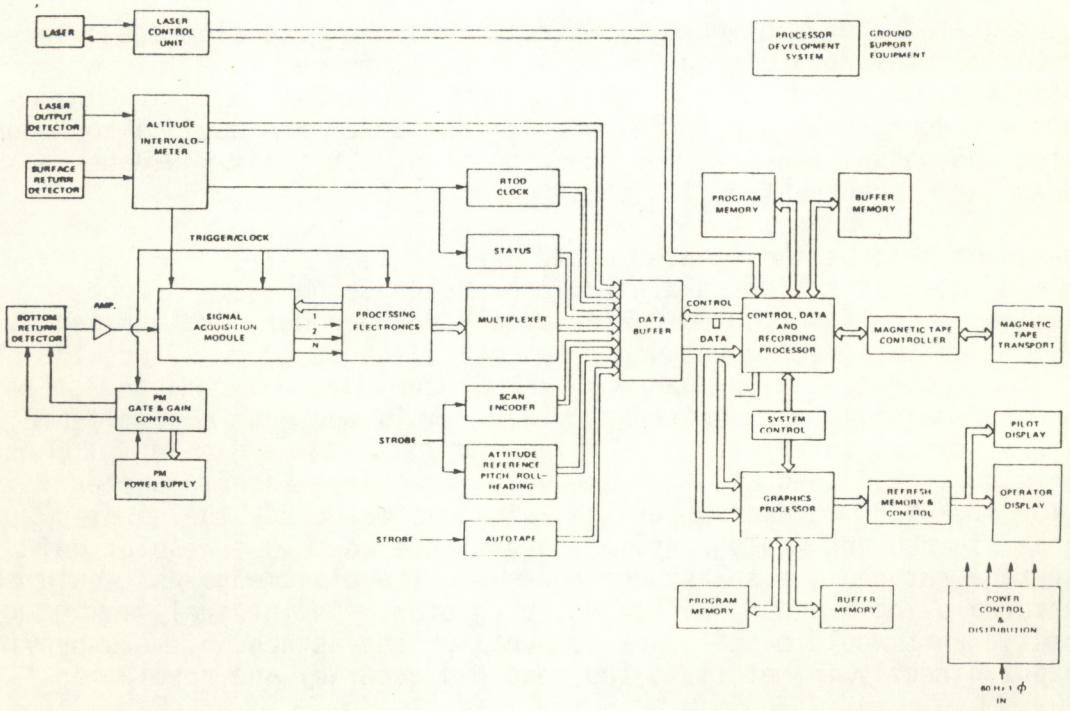

Figure 5-12. Electronics system block diagram.

5.3.1.2 Detectors

5.3.1.2.1 Laser Output Detector

To start the intervalometer process, the output of the laser must be detected at the instant the light exits the cavity. To perform this function, a fast detector with good sensitivity at the laser wavelength is required. The EG&G FND-100 photodiode has the appropriate characteristics and appears to be a good candidate for this application. Typical performance characteristics of this detector are shown in table 5-2.

The laser output also requires monitoring on a pulse-to-pulse basis for diagnostic purposes. A second FND-100 photodiode would be used to record a sample of the output energy over the laser pulse interval. This signal would be gated by the first detector onto an integrator and subseqently converted and recorded. This approach differs from that used in the AOL System where one detector was used to perform both tasks with some compromises in both functions. The method suggested here will allow an optimization of each function.

5.3.1.2.2 Surface Return Detector

The surface return detector will provide two important trigger functions required by the system: 1) a signal to stop the altitude intervalometer at the instant the surface return signal is detected and 2) a signal to initiate bottom return (bathymetry) acquisition and processing. To perform the function, a fast, AC-coupled photomultiplier having a gain of $\sim 10^6$ with good quantum efficiency at the laser wavelength is required.

Both 1/2" and 3/4" photomultipliers were assessed for this application. The 1/2" photomultipliers, although more convenient to use because of size, lacked the necessary rise time characteristics thereby leading to the selection of a 3/4" photomultiplier for the application. A good candidate is the RCA 8644. Pertinent characteristics of this photomultiplier are shown in table 5-3.

5.3.1.2.3 Bottom return detector

The bottom return detector must have several important characteristics. Because of the large expected dynamic range of the return signal, the unit should be gateable to allow rejection of the surface position of the signal return and yet have the capability to record subsurface returns. In addition, to maintain signal detection within the linear limits of the data acquisition electronics, it is desirable that the detector gain be time synchronized and logarithmically variable to provide increased gain as a function of depth to closely match and overcome the natural attenuation characteristics of the return signal. The detector must also possess the proper photocathode response rise time characteristics and quantum efficiency to satisfy the needs of this application. An assessment of available candidates has resulted in the selection of the ITT F4084 photomultiplier as the best choice to satisfy these requirements. Table 5-4 lists the characteristics of the device and figure 5-13 gives its typical grid gating response characteristics.

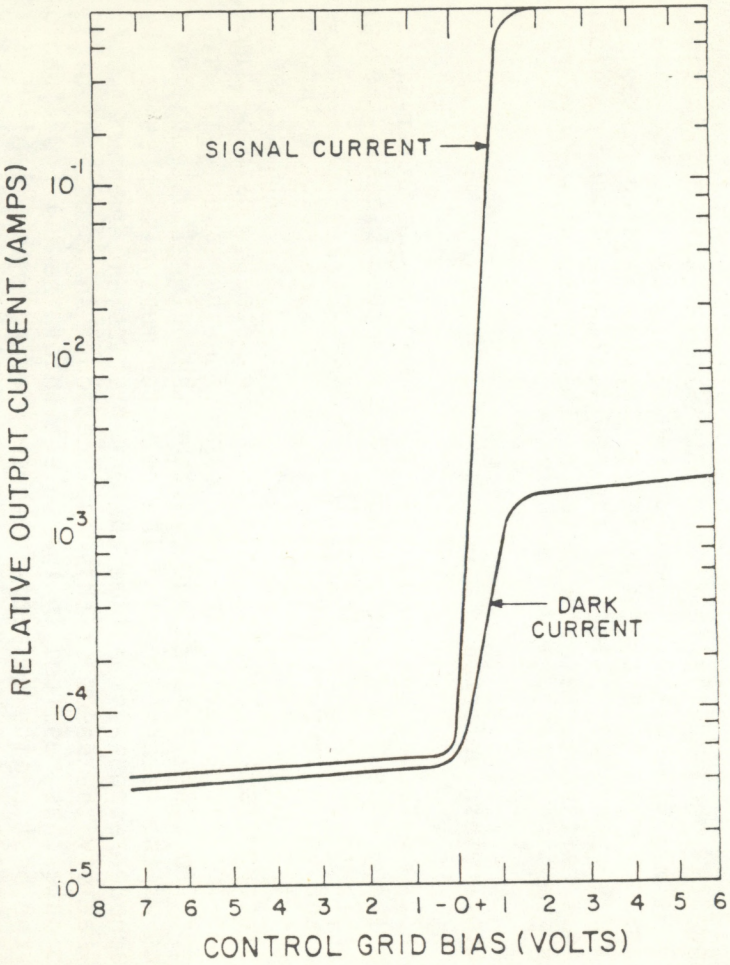

Figure 5-13. Typical grid gating characteristics of ITT F4084.

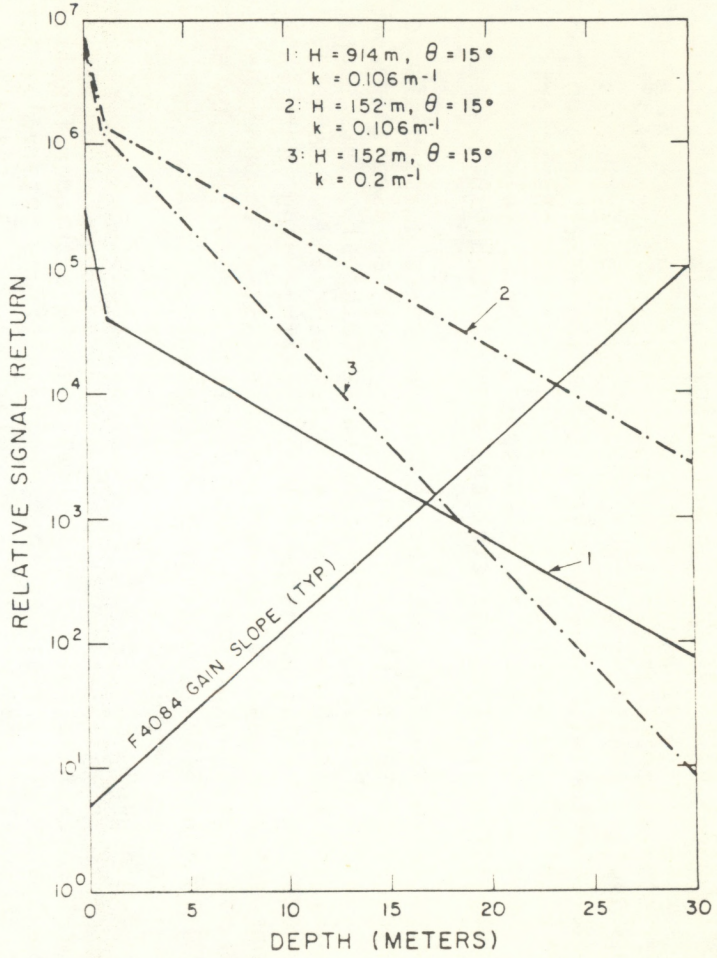

Figure 5-14. Signal return vs. depth.

As indicated in figure 5-13, the ITT F4084 can be controlled by applying a few volts of grid bias to the tube. This capability allows two important requirements to be satisfied: 1) gating and 2) time synchronized gain control. By applying 2 V of negative grid bias, the tube has a low gain; as the voltage is increased positively, the gain increases logarithmically. The primary function of the gate and gain control unit discussed in the next section is to systematically vary this grid voltage in accordance with the requirements of the specific measurement location.

5.3.1.2.3.1 Photomultiplier Gate and Gain Control

The ITT F4084 photomultiplier has several characteristics which can be employed to enhance the signal return detection process. The most important feature in this regard is its low voltage control grid which can be used to gate the tube on or off and control the gain by $\sim 5 \times 10^4$. To take full advantage of this capability, a gate and gain control function would be used to gate the tube off in between measurements and, by using programmable end points, set the initial and final gain to be utilized by the tube. Once triggered, the grid control bias would linearly integrate between the initial and final settings during the data taking interval. In this way, the gain requirements could be altered during setup to best match the characteristics of the surface and subsurface signal returns. Figure 5-14 shows the signal return characteristics as a function of depth for three representative cases. Case 1 indicates the predicted signal return at an altitude of 914 m, a scan angle of 15°, and an effective water attenuation coefficient, k, of 0.106 m^{-1}. Case 2 shows the effect of decreasing aircraft altitude to 152 m with all other parameters remaining the same, and Case 3 shows the effect of k being increased to 0.2 m^{-1}. A typical F4084 gain slope is also plotted on the figure to show that the tube has the capability to counteract the water attenuation characteristics and that a good match can be obtained by properly choosing the gain slope for various signal return conditions. In practice, this would be accomplished by setting the initial, end, and slope points in the gate and gain control unit for the best surface and bottom presentations for acquiring data in the area to be mapped.

A basic block diagram for the gate and gain control unit is shown in figure 5-15. The set points (initial, final, time constant) would be inputted through the system keyboard into the control processor and subsequently transferred to the appropriate registers. The two D/A converters would translate the digital values into analog voltages which would set the integrator end points. The time constant would be set by selecting one of n RC time constants. The integrator control trigger would initiate the integrator runup just prior to each signal return. This signal would be derived from the surface return detector and, by using an appropriate length of delay cable, would precede the signal by the proper time.

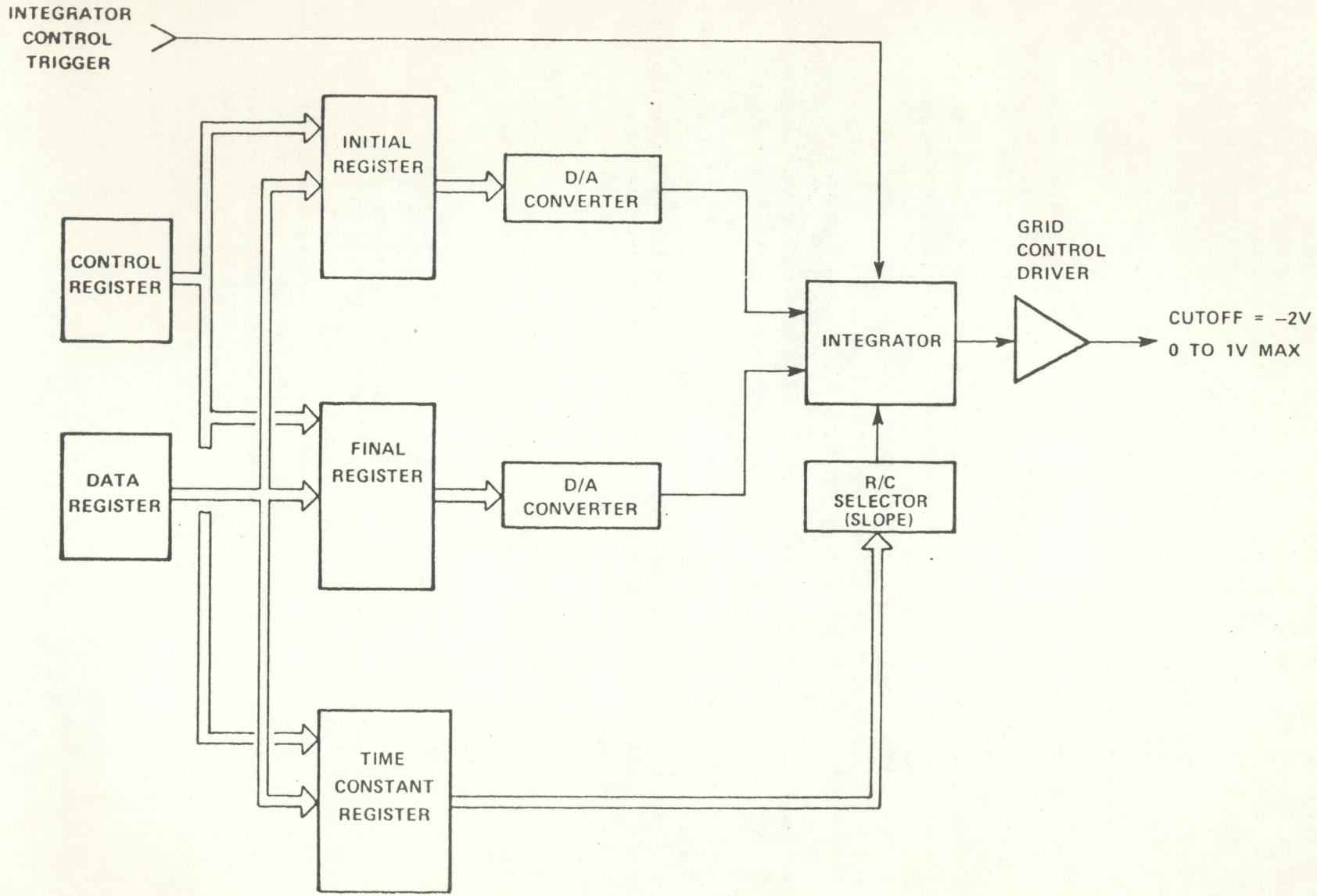

Figure 5-15. Gate and gain control block diagram.

5.3.1.2.4 Detector Power Supplies

Modular high voltage power supplies would be used to satisfy the surface and bottom return photomultiplier power requirements. These units are readily available from several manufacturers. The final choice of unit(s) would be made once the detailed packaging was complete and photomultiplier operating points had been determined. The laser output detector biases would be satisfied by power supplies incorporated into the processor control chassis.

5.3.1.3 Data Acquisition System

Certain aspects of the data acquisition system were privately developed by Avco Everett Research Laboratory, Inc., prior to initiation of efforts under Contract No. 7-35373. Although these aspects are included in the limited NOS airborne hydrography system to enhance the design, such information is regarded as proprietary. A functional description and some requirements of the system, however, are presented in sections 3.2.1 and 3.2.2.

5.3.1.4 Multiplexer and Data Buffer

A multiplexer and data buffer are required to control the data flow and momentarily store the information from the data acquisition system as well as ancillary support and housekeeping information.

A representative dataload for 1/10 and 2/10 sec. intervals, based on a data acquisition rate of 600 samples/sec. along with required housekeeping information, has been estimated and is shown in table 5-5. To reduce the interrupt overhead on the processors, two buffers, each having the capacity to store the acquired data, would be used alternately to momentarily store the information. The estimates shown in table 5-5 were prepared to approximate the buffer requirements; actual requirements would be determined during system detailed design. The latter shows, however, that the requirements can be satisfied with standard RAM memories (512 x 8 or 1024 x 8), that interrupt rates of 5 to 10 Hz (1/10 to 2/10 sec) are easily accomplished, and that the access rate is consistent with the information to be presented in real time (navigational grid deviations, course correction information, and pertinent housekeeping information). It also appears quite feasible to block data for recording by some multiple of the data buffer. Table 5-6 indicates the total estimated recording requirements based on the data and housekeeping information required for data processing and performance assessment purposes. Critical data flow paths would be software controlled to provide flexibility in the data collection and processing functions.

Table 5-5. Estimated data buffer requirements[1]

Item	# of Words	# of Bytes/ Word	1/10 sec Interval	2/10 sec Interval
Data (compressed)	60	2	120	240
Real Time of Day	10	6	60	120
Housekeeping	6	2	12	24
Attitude				
Pitch	6	2	12	24
Roll	6	2	12	24
Heading	6	2	12	24
Aircraft Position (1 Hz)	2	5	10	20
Intervalometer	60	2	120	240
Scanner	6	2	12	24
Status	1	2	2	4
Identification	32	2	64	64
Total			436 Bytes	874 Bytes

[1]Based on data acquisition rate of 600 samples/sec. plus required housekeeping information

Table 5-6. Estimated recording requirements

Item	# of Words	# of Bytes/ Word	Rate Samples/sec	Bytes/sec
Data (compressed)[1]	3	2	600	3600
Real Time of Day	1	6	100	600
Housekeeping	6	2	10	120
Attitude				
Pitch	1	2	60	120
Roll	1	2	60	120
Heading	1	2	60	120
Aircraft Position	2	5	1	10
Intervalometer	1	4	600	2400
Scanner	1	2	60	120
Status	1	2	10	20
Identification[2]	32	2		64
Total				7230

[1]Compressed mode provides depth and one variation between surface and expected bottom, if present

[2]Identification information appears only on header and trailer

5.3.1.5 Real-Time Processing

The real-time processing requirements for this application fall into two major categories: 1) mapping data and other support information must be properly formatted for recording on digital magnetic tape and 2) system and aircraft navigation information must be generated from the position fixing, attitude, heading and status data being collected to provide the system operator with overall performance information and the aircraft pilot with a display to aid him in flying a predetermined grid map. In conjunction with the grid map display, an on-course/off-course indication must be calculated and displayed for the pilot. The grid map deviation information will allow the flight crew to determine the area mapped relative to the planned area at any time during the flight, and the course indicator will enable the pilot to aline the aircraft on each flight leg or fill in voids should they occur.

Status information to assist the operator in determining mission performance will also be processed and displayed.

The most straightforward approach for fulfilling these requirements would be to employ two microprocessors (a control, data and recording processor, and a graphics processor, as is shown in figure 5-12), each dedicated to one of the major functions. The general approach would be to pass the appropriate information to each microprocessor after a "buffer-full" interrupt occurred and allow each to carry out its designated function.

5.3.1.5.1 Processor Section

The processor requirements for this application could be satisfied by either of two categories of these devices, an 8- or 16-bit MOS or bipolar microprocessor or a "minicomputer on a board." The bipolar microprocessor units would occupy less space and could perform all of the tasks required. The minicomputer on a board types require more space but are better supported with I/O hardware devices and more extensive vendor-supplied software. In order to make a final selection between the candidates, all I/O requirements, computational requirements, and the size and repetition rate would be carried out during detailed system design. The point here is that several units are available which could perform the required functions and, once the detailed information described above is available, the final selection of the appropriate device would be made.

Table 5-7 lists several microprocessors and minicomputers on a board which could perform the desired functions and would be considered in the final evaluation.

5.3.1.5.2 Software Development System

A software development system would be used to develop the system software, generate the grid map for each flight, and as a diagnostic tool during system maintenance and calibration. During hydrography system development, the software development system would be used to compile and assemble programs and to edit and debug the software. After the system programs and

routines have been developed, they would be transferred onto erasable PROM's and incorporated into the system processors. During flight planning, the software system would be used to generate the grid map for a particular area to be covered, and the information would then be transferred via magnetic tape to the hydrography system. Whenever maintenance or calibration activities were required, this unit could be attached to the system processors to provide these operations. It is expected that this unit would be considered as part of the normal hydrography system ground support equipment.

5.3.1.6 Recording

Hydrography data and support information for this application would be recorded on 9-track, 800-BPI digital magnetic tape. This will assure that the tape is compatible with most computing facilities and can be easily processed. An estimate of tape endurance, based on the recording requirements as delineated in table 5-6, is shown in table 5-8. Recording at 1600 BPI could also be considered and this would double the endurance shown in each case. However, the use of an 800-BPI record density lowers the risk of obtaining reliable recording in an aircraft environment and, unless a pressing need arises for greater tape endurance than that shown in table 5-8, 1600 BPI recording should not be employed.

5.3.1.7 Displays

The method used to assure that the desired area is completely covered during a mapping survey is very important in the utilization of systems of this type. Following determination of the area to be surveyed on a particular flight, a map or maps generated on the ground using the software development system would be displayed on the operator and pilot displays during flight. A navigation aid would also be provided to indicate to the pilot the leg or lane center to be flown during each data gathering pass. Deviations or gaps in the data collection process caused by difficulties in maintaining course would also be indicated on the displays to show which areas remain to be covered or require another pass.

To accomplish this function with the required resolution, a "refresh" memory type of display could be used. A display resolution of 256 x 256 is adequate to present the detail necessary for pilot and operator interpretation. An update rate of 1 to 3 times a second would be sufficient and quite compatible with the human response necessary to maintain and correct aircraft heading.

The display could also be used for diagnostic purposes to present raw signal returns to the operator for checkout, calibration, and performance verification purposes.

5.3.1.8 Timing

To correlate the data, positioning, and housekeeping information as well as any ancillary information which might be required, a real-time-of-day clock would be provided. The unit would be a 24-hour clock having a resolution of 0.1 msec. Clocks are now available which can provide this capability and naturally interface to the types of processors under consideration.

Table 5-7. Candidate processing devices

MICROPROCESSORS

Type	Manufacturer	Process	Word Size (Bits)
6801	Motorola	MOS	8
280	Zilog	MOS	8
28000	Zilog	MOS	16
mN601	Data General	MOS	16
10800	Motorola	ECL	4/slice
SBP9900	Texas Instruments	Bipolar	16

COMPUTER ON A BOARD

Type	Manufacturer	Process	Word Size (Bits)
Micronova	Data General	MOS	16
LSI-11/2	Digital	MOS	16
21MX-K	Hewlett Packard	SOS	16

Table 5-8. Estimated magnetic tape endurance

Tape Length (ft)	Tape Capacity M Bytes	Packing Factor	Estimated Endurance* (min)
2700	20	4:1	45
3600	27	4:1	60

*Continuous recording

Table 5-9. Vertical gyro characteristics

Item	Characteristic
Output	Pitch and roll
Time to Speed	3 min maximum
Roll Erection Rate	8°/min minimum between 30° and 5° of vertical
Pitch Erection Rate	15°/min minimum measured between 30° and 5° of vertical
Vertical Accuracy	0.1° rms to true vertical
Angular Error (Pitch and Roll)	$\pm 0.15^{\circ}$ rms to true pitch and roll
Pickoffs	Synchro output
Weight	2.3 lbs

5.3.1.9 Attitude Monitoring Unit

Several approaches were assessed to provide the pitch, roll, and heading information required for this application. The pitch and roll parameters must be known to an rms accuracy of 0.2^{o}. The first type of equipment investigated were units typically used for private aircraft. It was found that pitch and roll gyros can be obtained in this class of equipment which fall inside the 0.2^{o} requirement and are quite applicable.

Humphrey Inc., offers a vertical gyro which provides pitch and roll outputs in synchro form. Appropriate synchro-to-digital converters are available from several manufacturers which are easily interfaced to provide the information for processing purposes. Table 5-9 lists the characteristics of the Model VG36-0201-2 gyro which appears to be a good candidate for this application.

Heading must be known to an rms accuracy of 1^{o}. Private aircraft heading devices are available which use magnetic flux detection techniques and can provide the desired accuracy. The Humphrey Model DG11-01-07-1 directional gyro appears to be a good candidate for heading determination (see table 5-10).

The advantages in using these devices is in the cost saving over an attitude reference system which appears to be in the order of approximately 6:1. Volume, weight, and power requirements are also reduced which is important in small aircraft applications.

5.3.1.10 Aircraft Position Fixing Systems

To meet the requirements of this application, a means must be provided to determine the absolute position of the aircraft to an accuracy of less than 5 m over the area being surveyed. The assessment of positioning systems in ref. 9 was used to assist in determining which class and type of system would satisfy the needs here. After reviewing the characteristics and capabilities of several systems, it was decided that the Cubic Corp. DM40A Autotape appears to be the best choice for incorporation in the NOS Hydrography System. The specifications for this unit are shown in table 5-11. Its size, weight, and power consumption are compatible with small aircraft applications, and a digital interface is available for recording and is provided at the rate of once per second.

5.3.1.11 Mode Status and Housekeeping Data

Various mode and status points will be monitored throughout the system to provide performance information in real time. This data will also be recorded as a history of mode and operational performance throughout each mapping flight. Each mode or setting which could affect the data processing function would be included in the information recorded. Various housekeeping parameters would also be recorded to support data processing. This information would typically include detector power supply voltages which affect gain, laser power output, photomultiplier gain control settings, etc.

Table 5-10. Direction gyro characteristics

Item	Characteristic
Mechanical Freedom	
Inner Gimbal	$\pm 85^{\circ}$ minimum
Outer Gimbal	360° continuous
Accuracy (With Flux Detector)	1.0° rms
Pickoffs	Synchro output
Slaving Rate	0.5°/min minimum
Weight	3.3 lbs

Table 5-11. Aircraft position fixing system characteristics

Item	Characteristic
Operating Range	150 km
Range Accuracy	50 cm + 1:100,000 x range
Range Resolution	10 cm
Maximum Range Rate	160 nmi/hr
Display Rate	1/sec
Digital Output Rate	1/sec
Communications	Integral two way communications from interrogator to all responders
Data Outputs	20 line BCD (1, 2, 4, 8) for each range

Table 5-12. Electronics system size, power and weight estimates

Item	Est. Size Height/Width/Depth (inches)	Est. Weight (lbs)	Est. Power (watts)
Signal Acquisition Electronics	40/22/24	50	60
Autotape	11/19/21	55	95
Power Control and Distribution[1]	5.25/19/12	30	115
Magnetic Tape Transport	24/19/12	130	400
Process Controllers and Interface Electronics	12.25/19/21	60	575
Displays (2 each)	9.3/10/16	50	190
Laser Power, Control and Cooling	25/19/21	120	1650
Altitude Monitoring Unit[2]	-	-	40
Scanning Mirror Motor[2]	-	-	375
Electronics Racks (3 each)	40/22/24	180	-
Total		675 (306 kg)	3500

Notes: 1. Includes photomultiplier power supplies

2. Size and weight included in optical system estimates

5.3.1.12 Laser Control

A laser control unit would interface the laser to the processor which would command the laser to trigger at the desired rate. The timing and control logic to implement this function would be contained within this unit. Certain status information relative to laser operation would also be incorporated in this unit for display purposes.

5.3.1.13 Power Control and Distribution

A power control and distribution unit would provide the interface between aircraft power and the input power to the various system elements. The unit would contain line circuit breakers and individual unit circuit breakers. Input line filters would be included on the input power busses and, where required, line filters would be utilized on power lines to individual system elements. Lamps would indicate power availability from the busses and to the units. A system power-on timer would be included to indicate total operating time for equipment maintenance purposes.

5.3.1.14 Electronics System Size, Power, and Weight Estimates

Preliminary electronics system size, power, and weight estimates have been prepared and are listed in table 5-12. While the basic power available on the King Air aircraft will not satisfy the estimated 3.5 kW requirement, an optional AC inverter can be installed to provide the system needs.

5.3.1.15 Preliminary Electronics Rack Layout

A preliminary electronics rack layout is shown in figure 5-16. The installation of the racks in the King Air aircraft would be as depicted in figure 5-2.

5.3.2 Summary of Electronics System Performance Specifications

A summary of electronics system performance specifications is presented below.

A. Laser output detector

Responsivity at 532 nm	$\geq$ 0.3 A/W
Risetime	$\leq$ 1 nsec

B. Surface return detector

Quantum efficiency at 532 nm	$\geq$ 10 percent
Gain	$\approx 10^6$
Risetime	$\leq$ 1.5 nsec

C. Bottom return detector

Quantum efficiency at 532 nm	$\geq$ 10 percent
Gain	10^6, controllable over 4-5 decades
Gating	Required
Gate Time	< 5 nsec
Risetime	$\leq$ 1.5 nsec

D. Signal acquisition electronics

Risetime	< 1 nsec
Repetition rate	$\geq$ 600 Hz
Depth resolution	$\pm$ 0.3 m
Number of channels	100, to provide measurements from 0.3 to 30 m depth at a resolution of $\pm$ 0.3 m

E. Altitude intervalometer

Range	100 to 1000 m
Accuracy	$\pm$ 0.3 m
Resolution	$\pm$ 0.1 m

F. Attitude monitor

Heading accuracy	$\leq 1.0^{o}$
Pitch and roll accuracy	$\leq 0.2^{o}$
Output	Synchro

G. Aircraft position fixing

Operating range	150 km
Range accuracy	50 cm + 1:100,000 x range
Range resolution	10 cm
Maximum range rate	160 nmi/hr
Display rate	1/sec
Digital output rate	1/sec

H. Real time of day

Time frame	1/sec
Code output	Hours, minutes, seconds, milliseconds, 100's of microseconds
Resolution	100 μsec

I. Status — Critical system information to be chosen for recording and display

J. Housekeeping — Required data to be chosen for recording and display

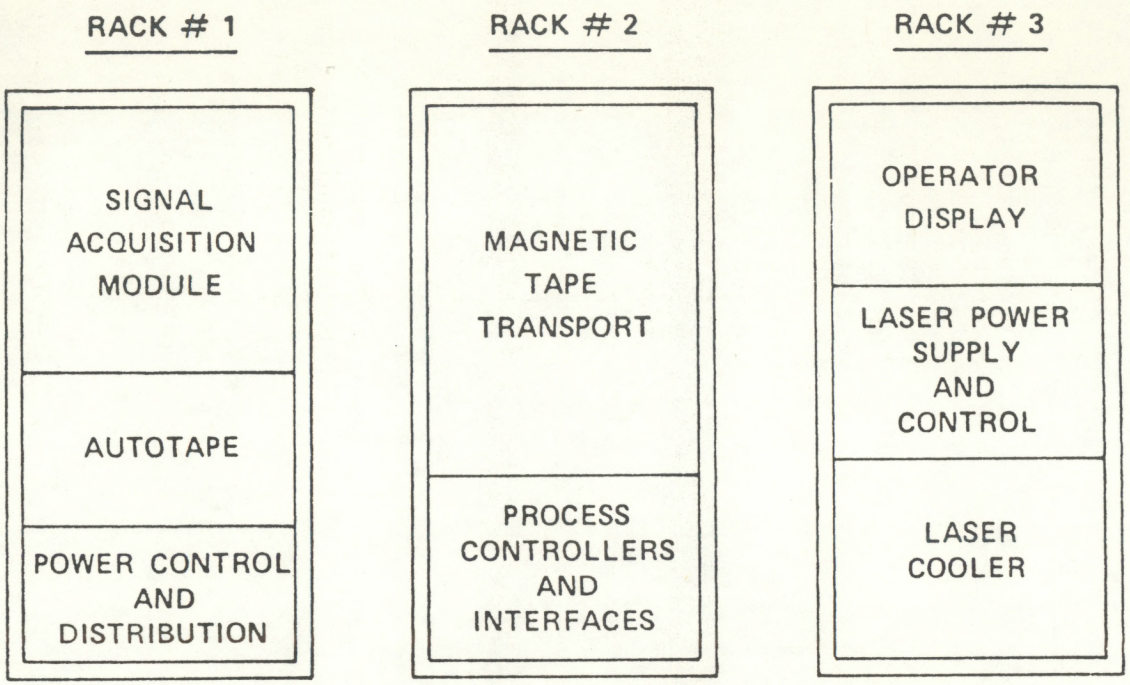

Figure 5-16. Preliminary electronics rack layout.

K. Control, data, and recording processor

1. Control functions
   a) Input laser commands
   b) Set initial, final and time constant for bottom return detector gate and gain control unit
   c) Set control parameters for signal acquisition
   d) Issue magnetic tape controller commands

2. Processing functions
   a) Format raw data for recording
   b) Perform data validation assessment
   c) Format system control commands into control codes

L. Graphics processor

1. Control functions
   a) Set display mode
   b) Issue refresh memory control commands

2. Processing functions
   a) Format raw data for operational pilot displays
      - navigation map
      - course deviations
      - data anomalies
      - course indicator

M. Processor development system

Purpose
   a) System software development
   b) System diagnostics
   c) Mission map development
   d) Quick-look data processing

N. Recorder

Format	9-track 800 BPI, industry compatible
Rate	45 IPS
Endurance	45 minutes continuous recording

O. Display

Type	Refresh memory - graphics
Format (graphics)	256 x 256 dot matrix
Character generation	5 x 7 dot matrix/character
Monitor	Compatible with American TV standards

5.4 Budgetary Estimates

Budgetary estimates of the labor and nonlabor (materials, travel, computing, etc.) were prepared for the implementation of the hydrography system design presented in this report and included documentation and engineering support to system operations subsequent to installation. The estimates are shown in table 5-13.

Table 5-13. Budgetary estimates

Item	Estimate
Labor	16,700 hrs.
Nonlabor	$360,000

It should be noted that the nonlabor element is unburdened and that no costs for aircraft modifications to accept the system have been included in the estimate. The budgetary estimate is for one system.

6. REFERENCES

[1]"Section F - Description/Specifications," U. S. Department of Commerce Contract No. 7-35373, September 30, 1977.

[2]Much of Jerlov's work is summarized in his recent book: N. G. Jerlov, Marine Optics, Elsevier Scientific Publishing Co., Amsterdam, 1976.

[3]Duntley, S. Q., "Underwater Lighting of Submerged Lasers and Incandescent Sources," SIO Ref: 71-1, Scripps Institute of Oceanography, University of California, San Diego, California, June 1971.

[4]Hass, M., and J. W. Davison, J. Opt. Soc. Amer. 67, 622 (1977).

[5]Clarke, G. L., and H. R. James, J. Opt. Soc. Amer., 29, 42 (1939).

[6]"Airborne Oceanographic Lidar System Final Report," Contract NAS6-2653, October 1975.

[7]"Prediction of Radar Range," L. V. Blake in Radar Handbook, M. I. Skolnik, editor, McGraw-Hill Book Co., New York (1970).

[8]"Department of Health, Education and Welfare Food and Drug Administration Laser Products Performance Standards," Fed. Reg. Vol. 40, No. 148.

[9]"Positioning Systems," Report on the Work of WG414b, presented at the SV International Congress of Surveyors, Stockholm, Sweden, June 1977.

(Continued from inside front cover)

NOS 16 Deep Sea Tide and Current Observations in the Gulf of Alaska and Northeast Pacific. Carl A. Pearson, December 1975.

NOS 17 Deep Sea Tide Observations Off the Southeastern United States. Carl A. Pearson, December 1975. (PB-250072)

NOS 18 Performance Evaluation of Guildline Model 8400 Laboratory Salinometer. James E. Boyd, July 1976.

NOS 19 Test Results on an Electromagnetic Current Sensor With an Open Design. David R. Crump, August 1976. (PB-260444)

NOS 20 Test and Evaluation of the Interocean Systems, Inc. Model 500 CTD/Oxygen pH In-Situ Monitor System. Barbara S. Pijanowski, August 1976. (PB-260442)

NOS 21 National Ocean Survey Abstracts - 1976. October 1977, 20 pp. (PB-275293)

NOS 22 Performance Evaluations of the Orbisphere Laboratories Models 2702 and 2709 Oxygen Measuring Systems. Jerald M. Peterson, Charles C. White, Barbara S. Pijanowski and Gary K. Ward, June 1979.

NOS 23 Performance Evaluation of the Martek Instruments, Inc. Mark V Digital Water Quality Analyzer System. Jerald M. Peterson, Charles C. White, Barbara S. Pijanowski and Gary K. Ward, June 1979.

NOS 24 Performance Evaluation of the Horiba Instruments, Inc. Model U-7 Water Quality Checker. Jerald M. Peterson, Charles C. White, Barbara S. Pijanowski and Gary K. Ward, June 1979. (PB-298815)

NOS 25 Technical Papers on Airborne Laser Hydrography (March - December 1978). Gary C. Guenther, Lowell R. Goodman, David B. Enabnit, Robert W.L. Thomas, and Robert N. Swift, June 1979.

NOS 26 The Cost Effectiveness of Airborne Laser Hydrography. David B. Enabnit, Lowell R. Goodman, G.K. Young and W.J. Shaughnessy, June 1979, 63 pp. (PB-299057)

NOAA SCIENTIFIC AND TECHNICAL PUBLICATIONS

The National Oceanic and Atmospheric Administration was established as part of the Depart Commerce on October 3, 1970. The mission responsibilities of NOAA are to assess the socioeconomic of natural and technological changes in the environment and to monitor and predict the state of the soli the oceans and their living resources, the atmosphere, and the space environment of the Earth.

The major components of NOAA regularly produce various types of scientific and technical i tion in the following kinds of publications:

PROFESSIONAL PAPERS — Important definitive research results, major techniques, and special investigations.

CONTRACT AND GRANT REPORTS — Reports prepared by contractors or grantees under NOAA sponsorship.

ATLAS — Presentation of analyzed data generally in the form of maps showing distribution of rainfall, chemical and physical conditions of oceans and atmosphere, distribution of fishes and marine mammals, ionospheric conditions, etc.

TECHNICAL SERVICE PUBLICATIONS — Reports containing data, observations, instructions, etc. A partial listing includes data serials; prediction and outlook periodicals; technical manuals, training papers, planning reports, and information serials; and miscellaneous technical publications.

TECHNICAL REPORTS — Journal quality with extensive details, mathematical developments, or data listings.

TECHNICAL MEMORANDUMS — Reports of preliminary, partial, or negative research or technology results, interim instructions, and the like.

Information on availability of NOAA publications can be obtained from:

ENVIRONMENTAL SCIENCE INFORMATION CENTER (D822)
ENVIRONMENTAL DATA AND INFORMATION SERVICE
NATIONAL OCEANIC AND ATMOSPHERIC ADMINISTRATION
U.S. DEPARTMENT OF COMMERCE

6009 Executive Boulevard
Rockville, MD 20852

NOAA--S/T 79-328